JOC The Journal of Organic Chemistry

pubs.acs.org/joc Article

Conformational Control of [2]Rotaxane by Hydrogen Bond

Yusuke Kawasaki, Showkat Rashid, Katsuhiko Ikeyatsu, Yuichiro Mutoh, Yusuke Yoshigoe, Shoko Kikkawa, Isao Azumaya, Shoichi Hosoya, and Shinichi Saito*

Cite This: J. Org. Chem. 2022, 87, 5744−5759 Read Online

ACCESS | Metrics & More | Article Recommendations | Supporting Information

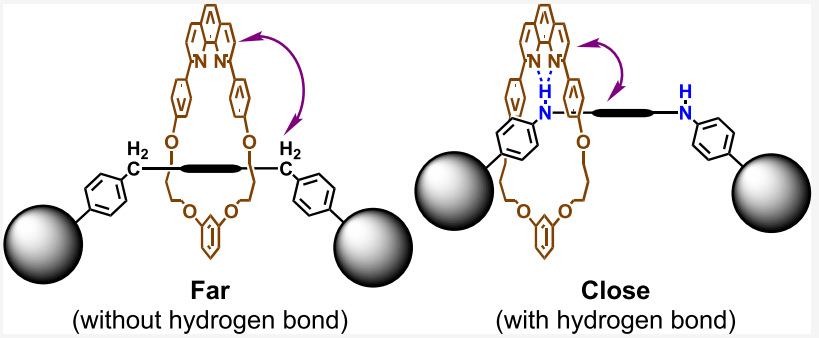

ABSTRACT: A series of [2]rotaxanes with various functional groups in the axle component was synthesized by the oxidative dimerization of alkynes, which is mediated by a macrocyclic phenanthroline−Cu complex. The rotaxanes were fully characterized by spectroscopic methods, and the structure of a rotaxane was determined by X-ray crystallographic analysis. The interaction between the ring component and the axle component was studied in detail to understand the conformation of the rotaxanes. The presence of the hydrogen bond between the phenanthroline moiety in the macrocyclic component and the acidic proton in the axle component influenced the conformation of rotaxane.

INTRODUCTION

[2]Rotaxane is an important class of interlocked compounds, and extensive studies related to the synthesis, structure, and dynamic behavior have been reported.[1] Following the seminal study of Dietrich−Buchecker and Sauvage, who reported the synthesis of [2]catenates from macrocyclic phenanthrolines by the metal-template method,[2] Gibson and co-workers reported the synthesis of [2]rotaxane based on a similar strategy.[3] These synthetic approaches were extensively applied to the synthesis of various interlocked compounds.[4]

Recent development of the synthetic methods related to interlocked compounds includes the use of a macrocyclic metal complex as a promotor for the bond-forming reaction. The metal-mediated reaction proceeded inside the macrocyclic metal complex so that the interlocked compounds could be synthesized efficiently.[5] Leigh and co-workers reported the first example of this approach, who employed a macrocyclic pyridine−Cu complex.[6] Assuming that the Cu complex could mediate coupling reactions such as the oxidative dimerization of alkynes (Glaser coupling), we reported the synthesis of [2]rotaxanes from macrocyclic phenanthroline−Cu complex and alkynes with bulky substituents (Scheme 1).[7] Interlocked compounds with polyyne structures have been synthesized by this method, and the properties of these compounds have been studied by several research groups.[8]

We have been interested in the conformation of [2]rotaxane with a macrocyclic phenanthroline ring. The phenanthroline moiety of the ring component would interact with the acidic hydrogen atom located in the axle component and the conformation of the [2]rotaxane could be affected, especially when the size of the ring component is small.[9] In this paper, we report the synthesis of small [2]rotaxanes with functionalized axle components (Scheme 2). The interaction between the ring and axle components was studied to understand the conformation of [2]rotaxanes.

RESULTS AND DISCUSSION

Synthesis of the Precursors for [2]Rotaxane. A macrocyclic phenanthroline−Cu complex (**2**) was synthesized by the reaction of **1**[8f] with CuI (Scheme 3). The reaction proceeded smoothly, and **2** was isolated in 61% yield.

As the precursor for the axle component, we designed a series of terminal alkynes with the tris(biphenyl)methyl group.

Received: January 14, 2022
Published: April 7, 2022

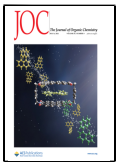

https://doi.org/10.1021/acs.joc.2c00086
J. Org. Chem. 2022, 87, 5744−5759

Scheme 1. Synthesis of [2]Rotaxane by Glaser Coupling[7a]

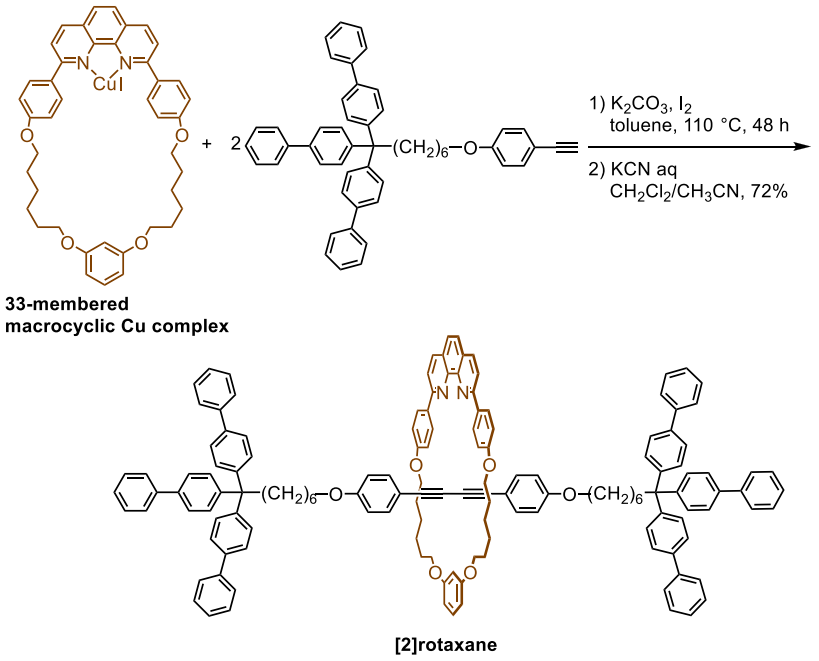

Scheme 2. Synthesis of Small [2]Rotaxanes with a Functionalized Axle Component

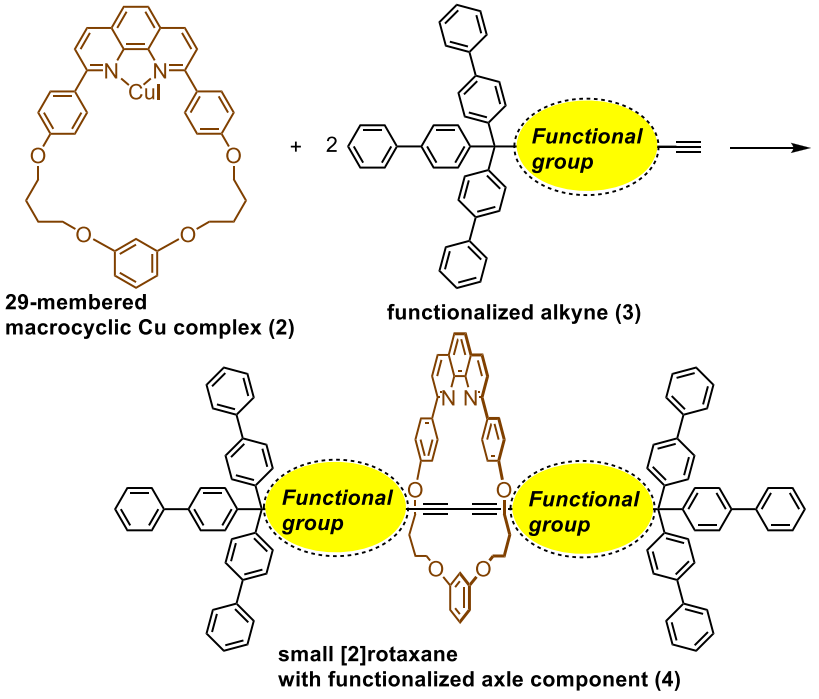

The syntheses of the alkynes **3a**–**i** are summarized in Schemes 4 and 5.

Tris([1,1′-biphenyl]-4-yl)methanol reacted with aniline hydrochloride under acidic conditions, and the substituted aniline **5**[10] was isolated in 64% yield (Scheme 4). Aniline **5** was converted to aryl iodide **6** by the Sandmeyer reaction.[11] Compound **6** was further converted to alkynes with various functional groups. For example, the Sonogashira reaction of **6** with (trimethylsilyl)acetylene and the removal of the trimethylsilyl (TMS) group gave **3a** in 83% yield. Similarly, the reaction of **6** with **7**[12] gave alkyne **3b** in comparable yield. Iodide **6** was converted to boronic acid **8** in 66% yield. The introduction of the benzyl group was achieved by the Suzuki–Miyaura reaction of **8** with 4-(trimethylsilylethynyl)benzyl bromide **9**.[13] The deprotection of **10** under basic conditions gave **3c** in 85% yield. An *N*-methylaniline derivative **11** was synthesized by the reaction of tris([1,1′-biphenyl]-4-yl)-methanol and *N*-methylaniline hydrochloride in 21% yield. Compound **11** reacted with iodide **12**[14] to give **13** in 76% yield,[15] and further removal of the TMS group gave **3d** in 63% yield.

Secondary amine **3f** was prepared by the Pd-catalyzed arylation of **5** and the removal of the TMS group (Scheme 5). Amide **3h** was synthesized by the condensation of **5** with acid

https://doi.org/10.1021/acs.joc.2c00086
J. Org. Chem. 2022, 87, 5744–5759

Scheme 3. Synthesis of Macrocyclic Cu(I)−Phenanthroline Complex 2

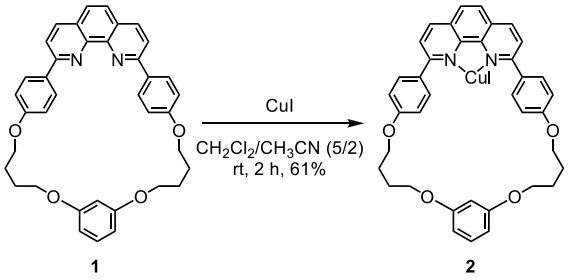

15.[16] The reduction of **3h** gave amine **3g** in a high yield. Fluorenylmethoxycarbonyl (Fmoc)-protected compound **3e** was synthesized by treating **3g** with FmocCl. Triazole derivative **3i** was prepared from **6** in three steps.[6]

Synthesis of [2]Rotaxanes. With the axle precursors in hand, we studied the synthesis of rotaxanes by the reaction of **2** with **3a−i**. The results are summarized in Table 1.

A mixture of phenanthroline−Cu complex **2** (1 equiv), alkyne **3a** (2.5 equiv), I_2 (1.0 equiv), and K_2CO_3 (10 equiv) in tetrahydrofuran (THF) was heated at 60 °C for 24 h. To the mixture was added I_2 (1.0 equiv) and K_2CO_3 (10 equiv), and the resulting mixture was heated again for 24 h. After the removal of the Cu ion by ammonia, product **4a** was isolated in 86% yield (entry 1, procedure A). Alkynes **3b** and **3c** were reacted with **2** under the same conditions, and [2]rotaxanes were isolated in 49% (**4b**) and 39% (**4c**) yields, respectively (entries 2 and 3). The yield of rotaxane decreased when **3d** was employed as the starting material (28%, entry 4). Rotaxane **4e** was isolated in 47% yield under modified conditions using smaller amounts of K_2CO_3 (3.75 equiv) and I_2 (1.25 equiv, entry 5, procedure B): to prevent the cleavage of the Fmoc group, KCN was used to remove the Cu ion. The synthesis of **4f** was examined under two reaction conditions, and the yield was better (60%) when procedure B was employed (entries 6 and 7). The reaction of benzylamine derivative **3g** gave the corresponding rotaxane **4g** in very low yield regardless of the procedures (entries 8 and 9). We assumed that the diarylamino group induced the removal of the copper ion from the phenanthroline moiety and suppressed the formation of rotaxane. Compound **4g** was synthesized in a better yield by the removal of the Fmoc group from **4e** (Scheme 6). Rotaxanes **4h** and **4i** were synthesized in 46% and 48% yields, respectively, by procedure A (entries 10 and 11).

The structure of **4a** was elucidated by X-ray crystallographic analysis, and the results are summarized in Figure 1. The molecular structure of **4a** provided insights into the conformation of the rotaxanes. In the molecular structure obtained by the recrystallization of **4a** from hexane−toluene, short contacts between the C_{sp} carbon atoms and the hydrogen atoms bound to the aromatic ring were observed (Figure 1a).[8f] We also succeeded in determining the molecular structure of

Scheme 4. Synthesis of Precursors 3a−d

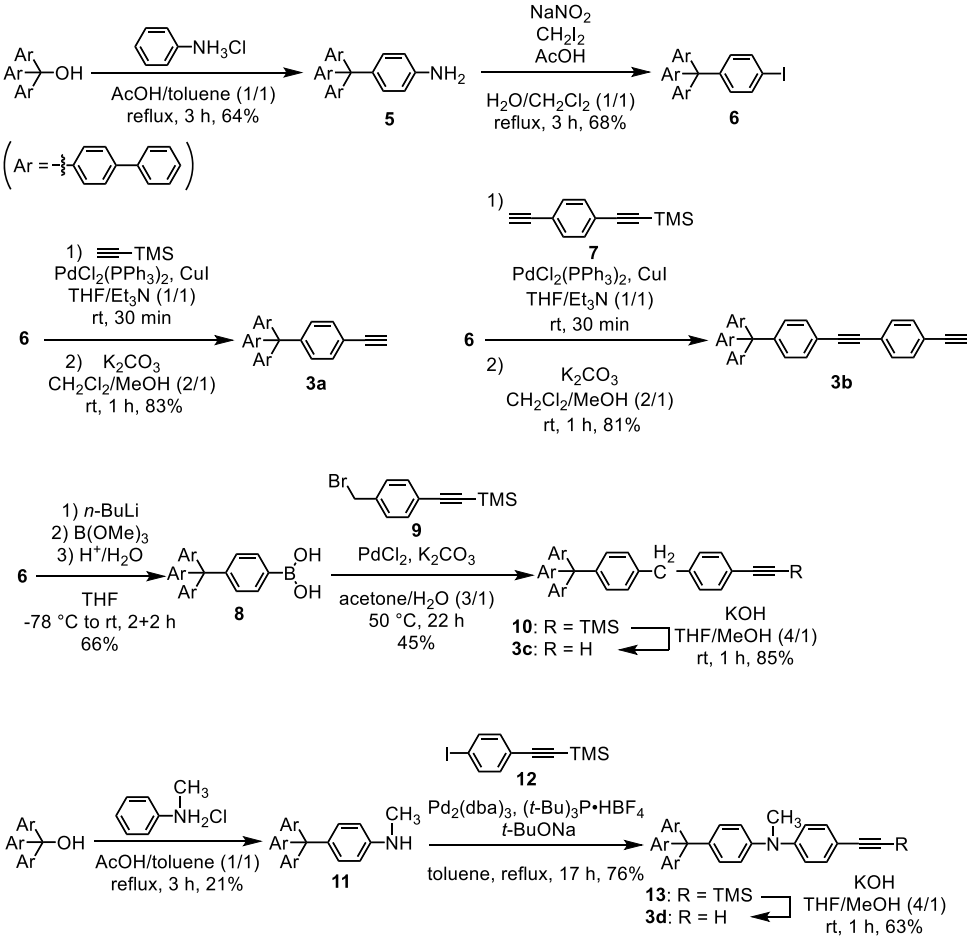

https://doi.org/10.1021/acs.joc.2c00086
J. Org. Chem. 2022, 87, 5744−5759

Scheme 5. Synthesis of Precursors 3e−i

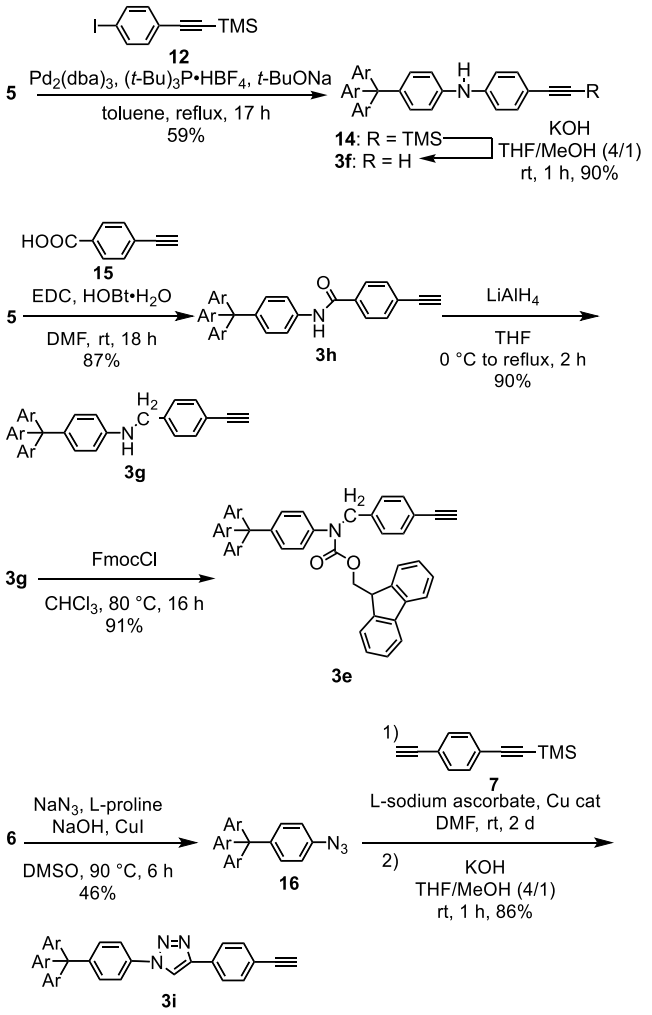

Table 1. Synthesis of a [2]Rotaxane 4 by Cu-Mediated Oxidative Coupling

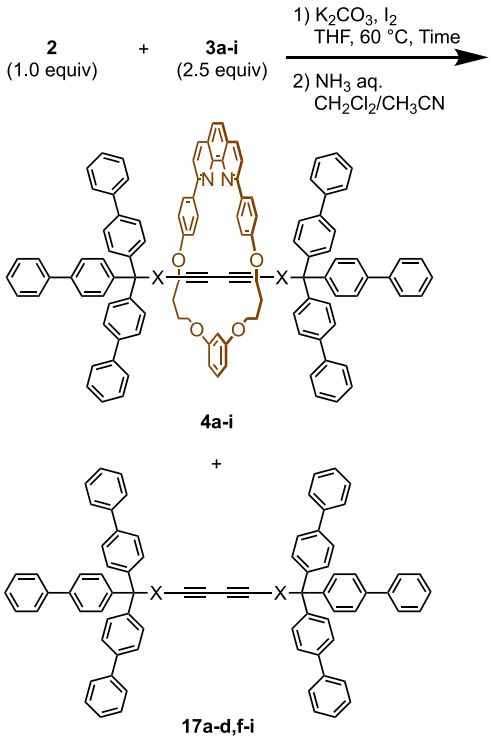

Entry	Alkyne	X	Rotaxane	Procedure[a]	Yield (%)
1	**3a**		**4a**	A	86
2	**3b**		**4b**	A	49
3	**3c**		**4c**	A	39
4	**3d**	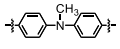	**4d**	A	28
5[b]	**3e**		**4e**	B	47
6	**3f**	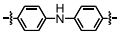	**4f**	A	24
7				B	60
8	**3g**	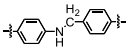	**4g**	A	6
9				B	0
10	**3h**	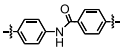	**4h**	A	46
11	**3i**		**4i**	A	48

[a]Procedure A: K_2CO_3 (10 + 10 equiv), I_2 (1.0 + 1.0 equiv), time (24 + 24 h); procedure B: K_2CO_3 (3.75 equiv), I_2 (1.25 equiv), time (48 h). [b]KCN was employed for the removal of the Cu ion.

4a from another sample, which was obtained by the recrystallization of **4a** from methyl *tert*-butyl ether (MTBE)−chloroform (Figure 1b). In the structure, the C−H···N interaction between chloroform and the phenanthroline moiety, in addition to the short contact between the C_{sp} carbon atom and the hydrogen atom, was detected (Figure 1b). A similar interaction has been reported in the literature.[17]

Comparison of the ^{1}H NMR Spectra of [2]Rotaxanes. Further analysis of the structure and conformation of [2]rotaxanes was done by ^{1}H NMR spectroscopy. In the spectra of [2]rotaxanes we studied, sharp signals were detected in most compounds and the localization of the ring component to a specific position was not observed at rt.[18,19] Based on these results, we assume that the movement of the ring component along the axle component is fast, and the observed chemical shifts are the average of the conformers. Partial ^{1}H NMR spectra of ring component **1** and [2]rotaxanes (**4a−i**) are shown in Figure 2. We assigned the signals[20] that correspond to H^d, H^e, and H^f of the macrocyclic components, and the chemical shifts were compared (Table 2). Based on the observed chemical shifts, rotaxanes were classified into two groups. In the compounds classified into group A (**4a−e**), the chemical shifts of H^d, H^e, and H^f appeared at 8.3−8.5, 7.1−7.2, and 7.0−7.1 ppm, respectively. It is noteworthy that the difference in the chemical shifts is small, regardless of the structure of the axle moiety. The chemical shifts of H^d and H^e in the phenanthroline moiety are similar to those of macrocyclic phenanthroline **1**, while the chemical shift of H^f, which is bound to the resorcinol framework, shifted downfield (0.4−0.5 ppm) compared to the corresponding signal of **1**. Because a larger difference of the chemical shift in the resorcinol moiety was induced by the formation of the [2]rotaxane, we assume that the "distance"[21] between the resorcinol moiety and the axle component is short: the axle

https://doi.org/10.1021/acs.joc.2c00086
J. Org. Chem. 2022, 87, 5744−5759

Scheme 6. Synthesis of [2]Rotaxane 4g by Deprotection of 4e

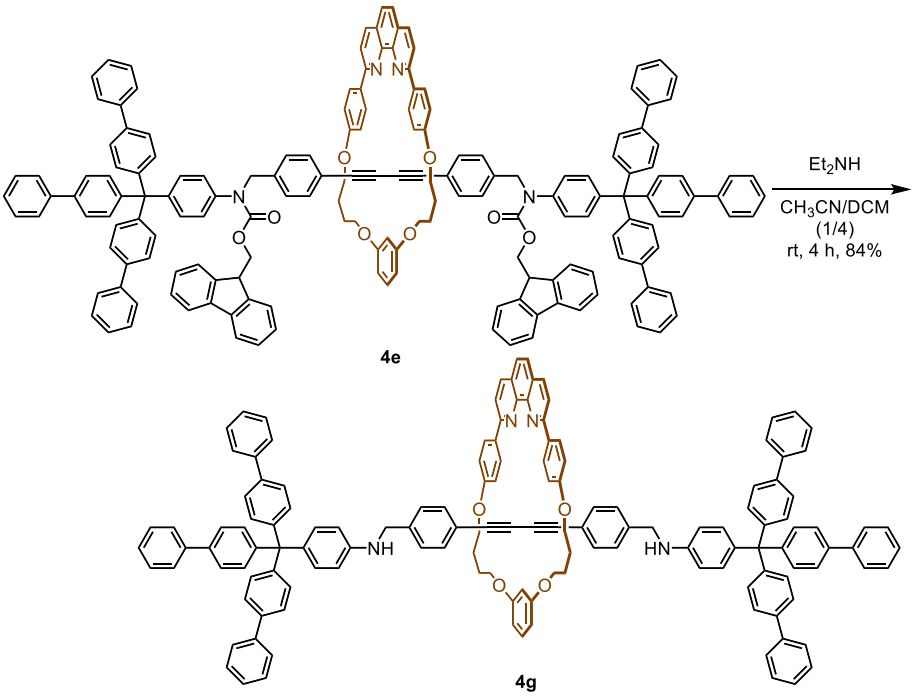

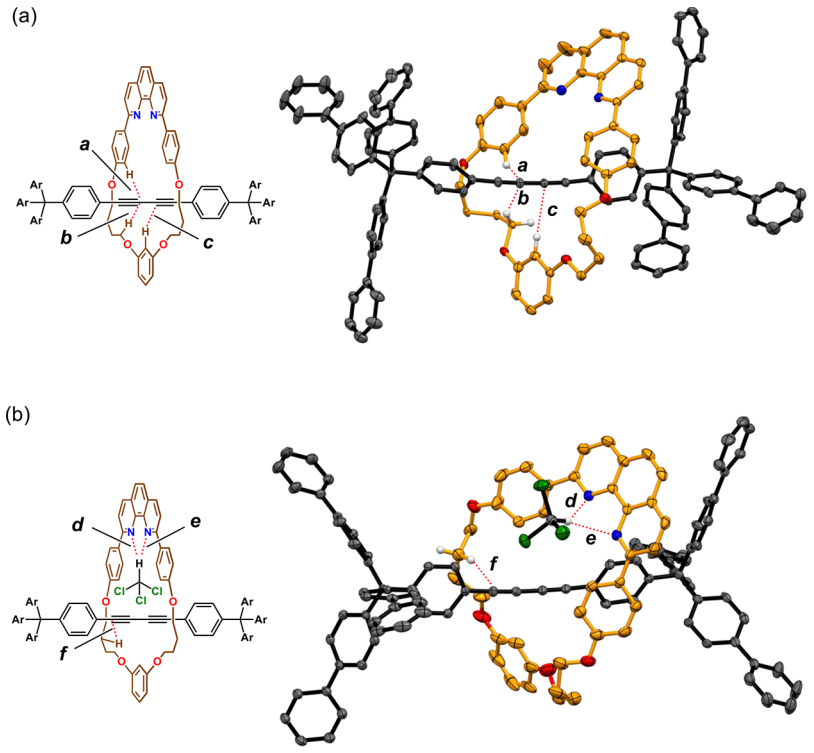

Figure 1. Molecular structure of [2]rotaxane **4a** with thermal ellipsoids at 50% probability. Most hydrogen atoms are omitted for clarity, and noncovalent interactions are shown by red dotted lines. (a) Sample obtained by recrystallization from hexane−toluene. Co-crystallized solvent molecules (toluene and hexane) are omitted for clarity. Only the position with higher occupancy of the disordered methylene groups is shown. d(CH/C_{sp}): (a) 2.80; (b) 2.79; (c) 2.79 Å. (b) Sample obtained by recrystallization from MTBE−chloroform. Only the position with higher occupancy of the disordered methylene and phenyl groups are shown. d(CH/N and CH/C_{sp}): (d) 2.32; (e) 2.50; (f) 2.70 Å.

component is not located in the proximity of the phenanthroline moiety.

In contrast, the chemical shifts (H^d, H^e, and H^f) of the compounds classified into group B (**4f–i**) were significantly different from those of **4a**. The chemical shifts of H^d and H^e in compounds that belong to group B shifted upfield compared to the corresponding chemical shifts of the compounds that belong to group A. For example, the chemical shift of H^d in **4a** appeared at 8.38 ppm, while the corresponding signal in **4f** appeared at 7.61 ppm.

https://doi.org/10.1021/acs.joc.2c00086
J. Org. Chem. 2022, 87, 5744−5759

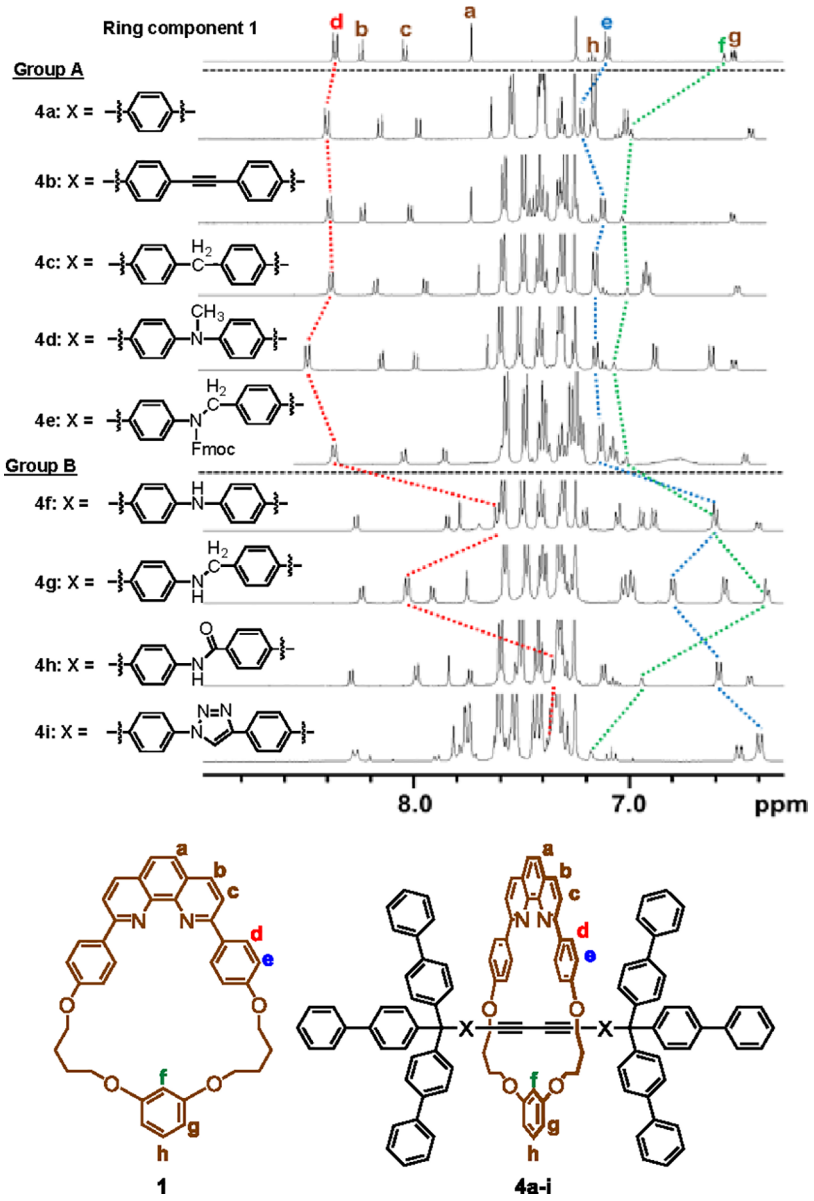

Figure 2. ^{1}H NMR spectra of [2]rotaxanes **4a**−**i** (500 MHz, $CDCl_3$, 295 K).

Furthermore, the difference in the chemical shifts strongly depends on the structure of the axle moiety, implying that the axle moiety is located in the proximity of the phenanthroline moiety. Next, we compared the chemical shifts of rotaxanes (**4**) with those of the corresponding axle components (**17**, Table 3). The difference between the chemical shifts of the methylene group (H^y) of **4c** and **17c** was small (ΔH^y = −0.19 ppm): in rotaxane **4c**, the signal appeared at 3.77 ppm, while the corresponding signal appeared at 3.96 ppm in **17c**. A similar trend was observed when we compared the chemical shift of the methyl group of **4d** with that of **17d**. The difference between the chemical shifts of the methyl group was small (ΔH^y = −0.16 ppm). Rotaxanes **4c** and **4d** belong to group A. When similar analyses were conducted with rotaxanes that belongs to group B, the difference in the chemical shifts was significantly large. The chemical shift (7.68 ppm) of the proton bound to the nitrogen atom in rotaxane (**4f**), for example, shifted upfield (5.87 ppm) in the axle component (**17f**): the difference in the chemical shifts was large (ΔH^y = 1.81 ppm). Similar results were obtained when we compared the chemical shifts of rotaxanes **4g**−**i** with diynes **17g**−**i**. The signal assigned to H^y in **4g**−**i** shifted upfield (1.03−1.67 ppm) in **17g**−**i**.

The results summarized in Tables 2 and 3 could be explained by assuming the presence (or absence) of the hydrogen bond between the axle component and the ring component of rotaxane. In **4c**, which belong to group A, no strong interaction between the axle component and the ring component would be present, and the axle component would be located in the proximity of the resorcinol moiety to minimize the steric interaction between the bulky phenanthroline moiety and the axle component (Figure 3). Consequently, the chemical shifts of H^d, H^e, and H^y are less affected by the presence of the axle component, while the signal of H^f shift downfield. The situation would change significantly in the rotaxanes that belong to group B.

In **4f**, for example, the presence of the hydrogen bond between the axle component and the ring component would affect the conformation of rotaxane (Figure 3). The axle

https://doi.org/10.1021/acs.joc.2c00086
J. Org. Chem. 2022, 87, 5744−5759

Table 2. Comparison of the Chemical Shifts (ppm) of [2]Rotaxanes 4a–i and the Ring Component 1[a]

Cmpd	Group	X	H^d	H^e	H^f	ΔH^d	ΔH^e	ΔH^f
1	-	-	8.36	7.10	6.55	-	-	-
4a	A		8.38	7.20	6.98	0.02	0.10	0.43
4b	A	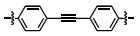	8.37	7.11	7.02	0.01	0.01	0.47
4c	A	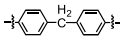	8.36	7.14	7.00	0.00	0.04	0.45
4d	A	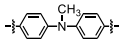	8.48	7.15	7.06	0.12	0.05	0.51
4e	A		8.35	7.14	7.00	-0.01	0.04	0.45
4f	B	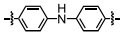	7.61	6.59	6.60	-0.75	-0.51	0.05
4g	B	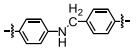	8.03	6.79	6.35	-0.33	-0.31	-0.20
4h	B	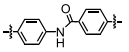	7.33	6.57	6.93	-1.03	-0.53	0.38
4i	B	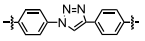	7.38	6.38	7.16	-0.98	-0.72	0.61

[a]$\Delta H^{d-f} = H^{d-f}(4) - H^{d-f}(1)$.

Table 3. Comparison of the Chemical Shifts (ppm) of [2]Rotaxanes 4c,d,f–i with the Axle Components 17c,d,f–i[a]

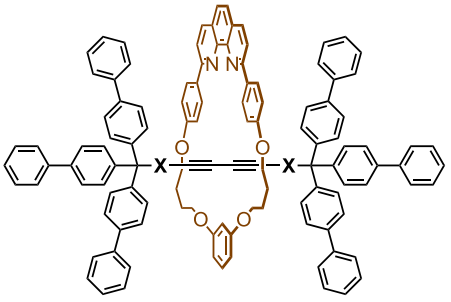

4c,d,f-i

Cmpd	Group	X	H^y	Diyne	H^y	ΔH^y
4c	A	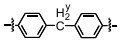	3.77	**17c**	3.96	-0.19
4d	A	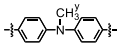	3.17	**17d**	3.33	-0.16
4f	B	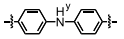	7.68	**17f**	5.87	1.81
4g	B	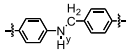	5.11	**17g**	4.08	1.03
4h	B	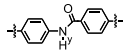	9.42	**17h**	7.75	1.67
4i	B	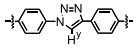	9.36	**17i**	8.19	1.17

[a]$\Delta H^y = H^y(4) - H^y(17)$.

component would be located in the proximity of the phenanthroline moiety. Consequently, the chemical shifts of H^d and H^e would be significantly affected by the presence of the axle component. The chemical shift of H^y would also be strongly affected by the presence of the macrocycle because H^y would form a hydrogen bond with the phenanthroline moiety.

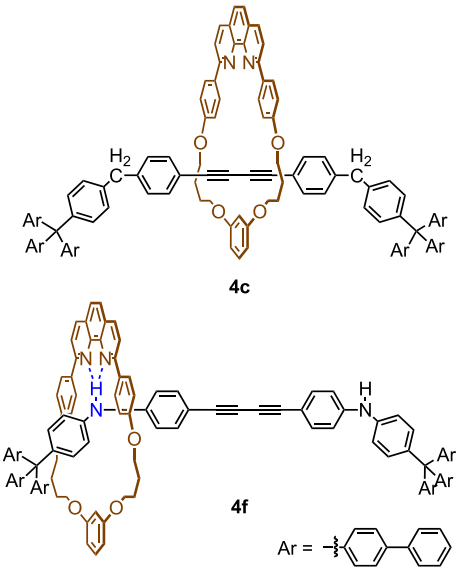

Figure 3. Supposed major conformation of **4c** and **4f** in $CDCl_3$.

The formation of the hydrogen bond between the acidic triazole proton and the amine moiety in [2]rotaxane has been postulated by several research groups.[22,23]

If the conformation of rotaxane was influenced by the presence of the hydrogen bond, a notable solvent effect on the chemical shifts of rotaxanes would be observed. In a highly polar solvent, the hydrogen bond between the axle component and the ring component would be cleaved, and this would affect the conformation as well as the chemical shifts of rotaxanes. To confirm the presence of the intramolecular hydrogen bond, we selected **4c**, in which the intramolecular hydrogen bond would not be present, and **4f**, in which the hydrogen bond between the phenanthroline moiety and the amino group would be present. We observed the ^1H NMR

https://doi.org/10.1021/acs.joc.2c00086
J. Org. Chem. 2022, 87, 5744–5759

spectra of **4c** and **4f** in two solvents (DMSO-d_6 and $CDCl_3$), and the results are shown in Figure 4. The chemical shifts of

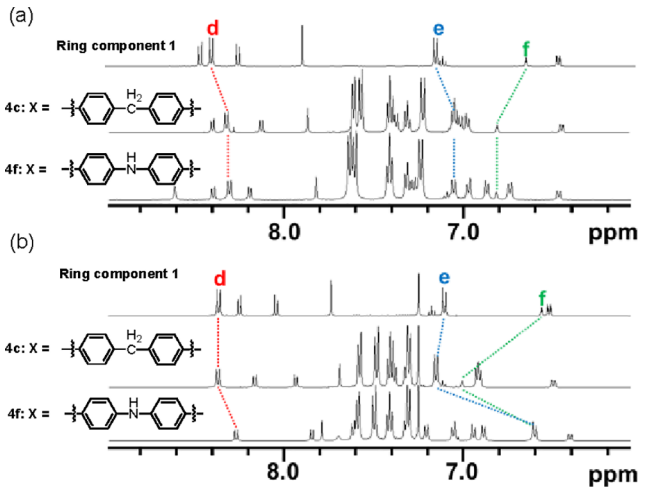

Figure 4. Partial ^{1}H NMR spectra of [2]rotaxanes **4c** and **4f** (500 MHz, 295 K); (a) in DMSO-d_6, (b) in $CDCl_3$.

rotaxanes **4c** and **4f** and ring component **1** are summarized in Table 4. When we observed the ^{1}H NMR spectra of **4c** and **4f**

Table 4. Comparison of Chemical Shifts (ppm) of [2]Rotaxanes 4c,f and Ring Component 1[a]

in DMSO-d_6

Cmpd	X	H^d	H^e	H^f	ΔH^d	ΔH^e	ΔH^f
1	–	8.41	7.17	6.67	–	–	–
4c	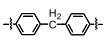	8.32	7.05	6.81	-0.09	-0.12	0.14
4f	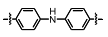	8.30	7.05	6.81	-0.11	-0.12	0.14

in $CDCl_3$

Cmpd	X	H^d	H^e	H^f	ΔH^d	ΔH^e	ΔH^f
1	–	8.37	7.10	6.57	–	–	–
4c	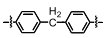	8.37	7.15	7.00	0.00	0.05	0.43
4f	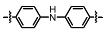	7.61	6.60	6.61	-0.76	-0.50	0.04

[a] $\Delta H^{d-f} = H^{d-f}(\mathbf{4}) - H^{d-f}(\mathbf{1})$.

in DMSO-d_6, the difference in the chemical shifts of H^d, H^e, and H^f was small (less than 0.2 ppm), implying that **4c** and **4f** would adopt a similar conformation in DMSO-d_6 (Table 4). Meanwhile, the ^{1}H NMR spectra of **4c** and **4f** were different in $CDCl_3$. In the NMR spectrum of **4c**, the signal of H^f shifted downfield (0.44 ppm) compared to the corresponding signal of macrocyclic phenanthroline **1**, and the difference in other signals (H^d and H^e) was negligible.[24]

The result implies that the axle component of **4c** is located in the proximity of the resorcinol moiety (Figure 3). In contrast, the chemical shifts of H^d and H^e shifted upfield (0.76 and 0.50 ppm, respectively) in **4f** compared to the corresponding signals of **1**, while the difference in the chemical shifts of H^f was small (0.04 ppm). The result could be explained by postulating the presence of the intramolecular hydrogen bond between the axle component and the ring component of **4f** (Figure 3). The axle component of **4f** would be located in the proximity of the phenanthroline moiety, and the chemical shifts of H^d and H^e would be strongly affected.

The presence of the intramolecular hydrogen bond was also supported by comparing the ^{1}H NMR chemical shifts of the axle moiety of rotaxanes and related compounds in different solvents (Table 5). The difference in the chemical shifts of the

Table 5. Comparison of the Chemical Shifts (ppm) of [2]Rotaxanes 4c,f and the Axle Components 17c,f[a]

Cmpd.	X	Solvent	H^y	Diyne	H^y	ΔH^y
4c	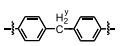	DMSO $-d_6$	3.73	**17c**	3.93	-0.20
4f	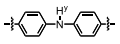	DMSO $-d_6$	8.61	**17f**	8.70	-0.09
4c		$CDCl_3$	3.77	**17c**	3.96	-0.19
4f		$CDCl_3$	7.68	**17f**	5.87	1.81

[a] $\Delta H^y = H^y(\mathbf{4}) - H^y(\mathbf{17})$.

methylene group of **4c** and that of **17c** in DMSO-d_6 was small (−0.20 ppm). Similar results were observed when the chemical shifts of the NH group of **4f** and that of **17f** in DMSO-d_6 were compared or the chemical shifts of the methylene group of **4c** and that of **17c** in $CDCl_3$ were compared. In contrast, a large difference (1.81 ppm) was observed when the chemical shifts of the NH group of **4f** and that of **17f** in $CDCl_3$ were compared. The results could be reasonably interpreted by postulating that the intramolecular hydrogen bond is present in a solution of **4f** in $CDCl_3$.[25]

Variable-Temperature ^{1}H NMR Experiments. We assumed that the conformation of [2]rotaxanes of group B adopted a structure with a low symmetry (Figure 3b). The observed NMR spectra at 295 K, however, do not directly correspond to the assumed conformation; the signals of the two dumbbell moieties, for example, were equivalent. The observed NMR spectra of [2]rotaxanes of group B could be explained in terms of the fast shuttling of the ring component at 295 K (Figure 5).[22,26]

Expecting that the rate of the shuttling would decrease at low temperatures and that the signals that reflect the less symmetric structure of [2]rotaxane would appear, we conducted the variable-temperature ^{1}H NMR experiments of **4c**, **4f**, and **4h** in CD_2Cl_2. When the ^{1}H NMR spectrum of **4c**, a negative control, was observed at low temperatures, only the broadening of the signals was observed, and the difference in the chemical shifts was small (Figure S1). Similar results were obtained when the ^{1}H NMR spectrum of **4f**, a rotaxane that would form a hydrogen bond, was recorded (Figure S2). In **4h**, on the other hand, the chemical shift of the amide group (H^y, 11.59 ppm) at 188 K was downfield (1.6 ppm) compared to the corresponding signal at 203 K (9.95 ppm, Figure 6). We assume that the signal observed at 203 K (9.95 ppm) split into two signals at a low temperature (188 K). One signal that appeared at 11.59 ppm would correspond to the amide proton that interacted with the phenanthroline moiety by the hydrogen bond, and the other signal was not detected because the signal overlapped with other signals.[27] Based on the observed data, the activation energy for the shuttling process of **4h** was assumed to be 8 kcal/mol.[28,29]

https://doi.org/10.1021/acs.joc.2c00086
J. Org. Chem. 2022, 87, 5744−5759

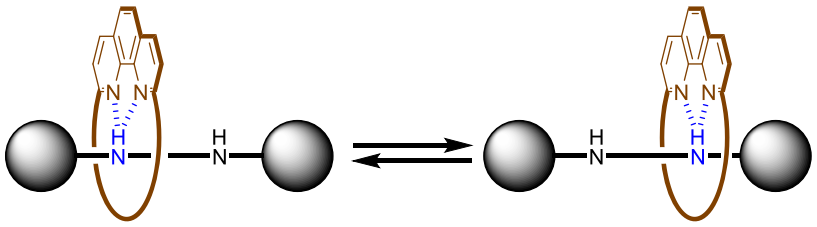

Figure 5. Expected shuttling behavior of group B rotaxanes.

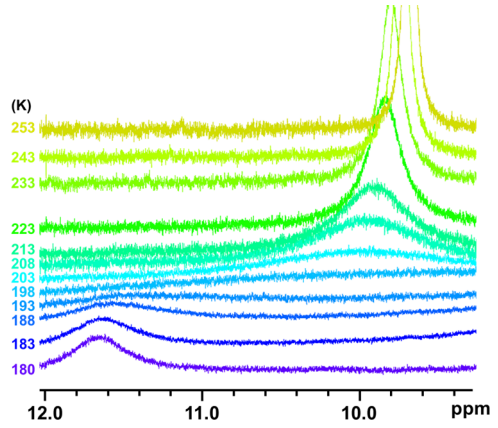

Figure 6. Partial VT ^{1}H NMR spectra of **4h** (500 MHz, CD_2Cl_2).

We anticipated that the N−H···N interaction would be stronger in a less polar solvent and observed the ^{1}H NMR spectra of **4f** in toluene-d_8 (Figure 7c, bottom). Notably, two NH signals were observed at 4.86 and 10.70 ppm at 193 K. We confirmed that these signals correspond to the amino group by observing the ^{1}H NMR spectra of the deuterated compound **4f-d_2** (78 atom % D of the N−D bond, Figure 7b, middle). Because the signal of the amino group of **17f** (the axle component of **4f**) was observed at 4.83 ppm in toluene-d_8 at 193 K (Figure 7a, top), the signal of **4f**, which appeared at 4.86 ppm, could be assigned to the free amino group, while the signal observed at 10.70 ppm would correspond to the amino group that interacted with the phenanthroline moiety. The amino groups in **4f** appeared as two non-equivalent signals at 193 K due to the decrease in the rate of the shuttling.[8h,30]

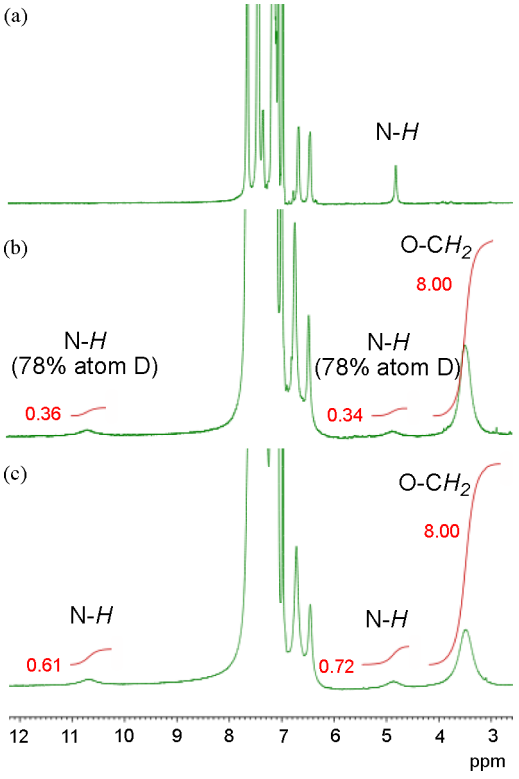

Figure 7. Partial ^{1}H NMR spectra of **4f** (bottom, c), **4f-d_2** (middle, b), and **17f** (top, a) at 193 K (400 MHz, toluene-d_8).

CONCLUSIONS

In summary, we synthesized [2]rotaxanes with various functional groups and studied the conformation of the compounds. The comparison of ^{1}H NMR spectra of [2]rotaxanes and related components in $CDCl_3$ showed that the spectra of rotaxanes were significantly affected by the structure of the axle component. The result could be explained by postulating the presence of the intramolecular hydrogen bond between the phenanthroline moiety and the acidic hydrogen atom in the axle component. The observation of some non-equivalent ^{1}H NMR signals at low temperatures supports the idea that the shuttling of the ring component occurs in some rotaxanes that form hydrogen bonds. The study would contribute to the understanding of the conformation of the interlocked compounds.

EXPERIMENTAL SECTION

General Methods. Reagents were commercially available and were used without further purification. An oil bath or a bead bath was used as the heat source, and the external temperature was reported. NMR spectra were recorded on a JEOL 400 or 500 MHz spectrometer or a Bruker 400 MHz NMR spectrometer. Chemical shifts were reported in delta units (δ) relative to chloroform (7.24 ppm for ^{1}H NMR and 77.0 ppm for ^{13}C NMR) or dimethyl sulfoxide (DMSO) (2.50 ppm for ^{1}H NMR and 39.5 ppm for ^{13}C NMR). Multiplicity is indicated by s (singlet), d (doublet), t (triplet), q (quartet), quint (quintet), m (multiplet), or br (broad). Coupling constants, J, are reported in Hertz. IR spectra were recorded on a Fourier transform infrared spectrometer using a diamond ATR module. A YMC-GPC T30000 (21.2 mm ID × 600 mm L) column was used for GPC separation using $CHCl_3$ as the eluent. Thin layer chromatography was performed on Merck silica gel 60F-254 plates. Column chromatography was performed using Kanto Chemical silica gel 60N (spherical, neutral 40−50 μm). High-resolution mass spectra (HRMS) were obtained by using a time-of-flight (TOF) mass analyzer.

*Macrocyclic Cu(I)−Phenanthroline Complex (**2**).* To a solution of **1**[8f] (408 mg, 0.70 mmol) in CH_2Cl_2 (35 mL) was added a solution of CuI (133 mg, 0.70 mmol, 1 equiv) in CH_3CN (14 mL), and the mixture was stirred at rt for 2 h. The solvent was removed in vacuo, and the residue was recrystallized from hexane−CH_2Cl_2 to yield **2** (328 mg, 0.42 mmol, 61%) as an orange powder: mp 171.1−172.2

https://doi.org/10.1021/acs.joc.2c00086
J. Org. Chem. 2022, 87, 5744−5759

°C; ^{1}H NMR (400 MHz, $CDCl_3$): δ 8.44 (d, *J* = 7.6 Hz, 2H), 8.02 (br, 8H), 7.13 (m, 5H), 7.10 (t, *J* = 8.6 Hz, 1H), 6.59 (s, 2H), 6.47 (d, *J* = 8.4 Hz, 2H), 4,29 (t, *J* = 6.2 Hz, 4H), 4.03 (s, 4H), 2.06 (br, 4H), 1.93 (br, 4H); $^{13}C\{^1H\}$ NMR (100 MHz, DMSO-d_6, 423 K): δ 161.0, 160.9, 160.7, 144.6, 138.1, 130.6, 130.5, 130.3, 126.9, 126.7, 116.3, 108.1, 103.2, 79.6, 68.8, 26.3, 26.1 (one signal is missing); IR (ATR): 1603, 1582, 1487 cm^{-1}; Anal. Calcd for $C_{38}H_{34}CuIN_2O_4 \cdot 1.6(CH_2Cl_2)$: C, 52.32; H, 4.12; N, 3.08. Found: C, 52.38; H, 3.73; N, 3.01.

*4-[Tris([1,1′-biphenyl]-4-yl)methyl]iodobenzene (**6**).* A mixture of 4-[tris([1,1′-biphenyl]-4-yl)methyl]aniline **5**[10] (2.82 g, 5.0 mmol), $NaNO_2$ (1.73 g, 25 mmol, 5 equiv), CH_2I_2 (2.68 g, 10 mmol, 2 equiv), CH_2Cl_2 (50 mL), and H_2O (25 mL) was stirred at rt for 5 min under Ar. After the addition of acetic acid (6.01 g, 100 mmol, 20 equiv), the mixture was refluxed for 3 h, cooled to rt, and extracted with CH_2Cl_2 (3 × 30 mL). The combined organic layer was washed with water, dried over $MgSO_4$, and concentrated in vacuo. The residue was purified by silica gel column chromatography (hexane/CH_2Cl_2 = 5/1) to yield **6** (2.26 g, 3.4 mmol, 68%) as a colorless solid; mp 215.7−218.4 °C; ^{1}H NMR (500 MHz, $CDCl_3$): δ 7.61 (d, *J* = 9.2 Hz, 2H), 7.59 (d, *J* = 8.0 Hz, 6H), 7.51 (d, *J* = 8.0 Hz, 6H), 7.41 (t, *J* = 8.0 Hz, 6H), 7.30−7.33 (m, 9H), 7.08 (d, *J* = 7.5 Hz, 2H); $^{13}C\{^1H\}$ NMR (100 MHz, $CDCl_3$): δ 146.6, 145.2, 140.4, 138.8, 136.7, 133.2, 131.3, 128.8, 127.3, 127.0, 126.3, 91.9, 64.1; IR (ATR): 1484 cm^{-1}; HRMS (FAB): calcd for $C_{43}H_{31}I$ ($[M]^+$), 674.1470; found, 674.1468.

*4-[Tris([1,1′-biphenyl]-4-yl)methyl]ethynylbenzene (**3a**).* A mixture of **6** (421 mg, 0.62 mmol), $Pd[(PPh_3)_2]Cl_2$ (13.1 mg, 0.019 mmol, 3.0 mol %), and CuI (7.1 mg, 0.037 mmol, 6.0 mol %) in dry THF (10 mL) and dry triethylamine (10 mL) was stirred at rt for 5 min under Ar. (Trimethylsilyl)acetylene (0.10 mL, 0.72 mmol, 1.2 equiv) was added in one portion, and the mixture was stirred at rt for 30 min. Saturated NH_4Cl aq (10 mL) was poured into the solution, and the mixture was extracted with MTBE (3 × 30 mL). The combined organic layer was washed with brine, dried over Na_2SO_4, and concentrated in vacuo. To the residue were added K_2CO_3 (172 mg, 1.3 mmol, 2.0 equiv), CH_2Cl_2 (20 mL), and MeOH (10 mL), and the mixture was stirred at rt for 1 h. After the addition of water, the mixture was extracted with CH_2Cl_2 (3 × 25 mL). The combined organic layer was washed with water, dried over $MgSO_4$, and concentrated in vacuo. The residue was purified by silica gel column chromatography (hexane/CH_2Cl_2 = 5/1) to yield **3a** (298 mg, 0.52 mmol, 83%) as a white solid; mp 232.8−234.6 °C; ^{1}H NMR (500 MHz, $CDCl_3$): δ 7.59 (d, *J* = 7.5 Hz, 6H), 7.52 (d, *J* = 8.6 Hz, 6H), 7.40−7.45 (m, 8H), 7.30−7.34 (m, 11H), 3.05 (s, 1H); $^{13}C\{^1H\}$ NMR (126 MHz, $CDCl_3$): δ 147.6, 145.3, 140.4, 138.8, 131.44, 131.39, 131.0, 128.8, 127.3, 127.0, 126.3, 119.7, 83.5, 77.1, 64.3; IR (ATR): 1486 cm^{-1}; HRMS (ESI): calcd for $C_{45}H_{32}$ ($[M]^+$), 572.2499; found, 572.2496.

*4-[Tris([1,1′-biphenyl]-4-yl)methyl]-([4-ethynylphenyl]ethynyl)-benzene (**3b**).* A mixture of **6** (337 mg, 0.5 mmol), $Pd[(PPh_3)_2]Cl_2$ (10.5 mg, 0.015 mmol, 3.0 mol %), and CuI (5.71 mg, 0.030 mmol, 6.0 mol %) in dry THF (10 mL) and dry triethylamine (10 mL) was stirred at rt for 5 min. To the mixture was added ([4-ethynylphenyl]-ethynyl)trimethylsilane **7** (99.2 mg, 0.5 mmol, 1.0 equiv), and the resulting mixture was stirred for 30 min. The mixture was added to a saturated aqueous solution of NH_4Cl (10 mL) and extracted with MTBE (3 × 30 mL). The combined organic layer was washed with brine, dried over Na_2SO_4, and concentrated in vacuo; To the residue was added K_2CO_3 (138 mg, 1.0 mmol, 2.0 equiv), CH_2Cl_2 (20 mL), and MeOH (10 mL), and the mixture was stirred at rt for 1 h. After the addition of water, the mixture was extracted with CH_2Cl_2 (3 × 25 mL). The combined organic layer was washed with water, dried over $MgSO_4$, and concentrated in vacuo. The residue was purified by silica gel column chromatography (hexane/CH_2Cl_2 = 5/1) to yield **3b** (273 mg, 0.41 mmol, 81%) as a white solid; mp 238.8−240.4 °C; ^{1}H NMR (500 MHz, $CDCl_3$): δ 7.61 (d, *J* = 7.5 Hz, 6H), 7.53 (d, *J* = 8.6 Hz, 6H), 7.41−7.47 (m, 12H), 7.31−7.37 (m, 11H), 3.15 (s, 1H); $^{13}C\{^1H\}$ NMR (126 MHz, $CDCl_3$): δ 147.4, 145.4, 140.4, 138.8, 132.0, 131.5, 131.4, 131.1, 130.9, 128.8, 127.3, 127.0, 126.3, 123.8, 121.8, 120.5, 91.2, 89.0, 83.3, 78.9, 64.3; IR (ATR): 1512, 1486 cm^{-1}; HRMS (ESI): calcd for $C_{53}H_{36}$ ($[M]^+$), 672.2812; found, 672.2803.

*4-[Tris([1,1′-biphenyl]-4-yl)methyl]phenylboronic Acid (**8**).* A mixture of **6** (880 mg, 1.3 mmol) in dry THF (8 mL) was cooled to −78 °C under Ar. Then, *n*-BuLi in hexane (1.00 mL, 1.57 M, 1.56 mmol, 1.2 equiv) and $B(OMe)_3$ (0.35 mL, 0.33 mmol, 2.4 equiv) were added, and the mixture was stirred for 2 h. The mixture was allowed to warm to rt and stirred again for 2 h. Saturated NH_4Cl aq (10 mL) was poured into the reaction mixture, and the resulting mixture was stirred for 5 min and extracted with MTBE (3 × 20 mL). The combined organic layer was washed with water, dried over $MgSO_4$, and concentrated in vacuo. The residue was purified by silica gel column chromatography (hexane/CH_2Cl_2 = 1/2) to yield **8** (510 mg, 0.86 mmol, 66%) as a colorless amorphous solid; mp 231.1−232.7 °C; ^{1}H NMR (500 MHz, DMSO-d_6): δ 8.03 (s, 2H), 7.75 (d, *J* = 8.6 Hz, 2H), 7.66−7.69 (m, 12H), 7.45 (t, *J* = 8.0 Hz, 6H), 7.34−7.37 (m, 9H), 7.26 (d, *J* = 8.6 Hz, 2H); $^{13}C\{^1H\}$ NMR (100 MHz, DMSO-d_6): δ 149.7, 147.1, 141.0, 139.2, 135.3, 133.5, 132.6, 131.1, 130.5, 129.0, 128.1, 127.6, 65.6; IR (ATR): 1485 cm^{-1}; Anal. Calcd for $C_{43}H_{33}BO_2$ (−1/6 H_2O): C, 87.61; H, 5.59. Found: C, 87.68; H, 5.59.

*4-[Tris([1,1′-biphenyl]-4-yl)methyl]-(4-[trimethylsilyl]-ethynylbenzyl)benzene (**10**).* To a mixture of **8** (398 mg, 0.67 mmol), [(4-[bromomethyl]phenyl)ethynyl]trimethylsilane **9** (179 mg, 0.67 mmol, 1.0 equiv), K_2CO_3 (232 mg, 1.7 mmol, 2.5 equiv), acetone (5.1 mL), and water (1.7 mL) was added $PdCl_2$ (2.01 mg, 0.011 mmol, 1.7 mol %) at rt under Ar with stirring. The mixture was heated to 50 °C for 22 h. The solvent was cooled to rt and extracted with CH_2Cl_2 (3 × 20 mL). The combined organic layer was dried over Na_2SO_4 and concentrated in vacuo. The residue was purified by silica gel column chromatography (hexane/CH_2Cl_2 = 3/1) to yield **10** (224 mg, 0.31 mmol, 45%) as a white solid; mp 237.5−239.9 °C; ^{1}H NMR (500 MHz, $CDCl_3$): δ 7.59 (d, *J* = 7.5 Hz, 6H), 7.51 (d, *J* = 8.0 Hz, 6H), 7.38−7.42 (m, 8H), 7.30−7.34 (m, 9H), 7.22 (d, *J* = 8.0 Hz, 2H), 7.14 (d, *J* = 8.0 Hz, 2H), 7.07 (d, *J* = 8.0 Hz, 2H), 3.94 (s, 2H), 0.23 (s, 9H); $^{13}C\{^1H\}$ NMR (100 MHz, $CDCl_3$): δ 145.9, 144.6, 141.6, 140.5, 138.6, 138.3, 132.1, 131.5, 131.2, 128.9, 128.7, 128.0, 127.2, 126.9, 126.1, 120.9, 105.1, 93.7, 64.0, 41.4, 0.0; IR (ATR): 1618, 1508, 1484 cm^{-1}; HRMS (FAB): calcd for $C_{55}H_{46}Si$ ($[M]^+$), 734.3369; found, 734.3368.

*4-[Tris([1,1′-biphenyl]-4-yl)methyl]-(4-ethynylbenzyl)benzene (**3c**).* A mixture of **10** (184 mg, 0.25 mmol), KOH (21.0 mg, 0.38 mmol, 1.5 equiv), MeOH (2.4 mL), and THF (9.6 mL) was stirred at rt for 1 h. To the solution was added water, and the mixture was extracted with EtOAc (3 × 20 mL). The combined organic layer was washed with brine, dried over Na_2SO_4, and concentrated in vacuo. The residue was purified by silica gel column chromatography (hexane/CH_2Cl_2 = 3/1) to yield **3c** (140 mg, 0.21 mmol, 85%) as a white solid; mp 210.0−212.4 °C; ^{1}H NMR (500 MHz, $CDCl_3$): δ 7.59 (d, *J* = 8.0 Hz, 6H), 7.51 (d, *J* = 6.9 Hz, 6H), 7.39−7.42 (m, 8H), 7.30−7.35 (m, 9H), 7.23 (d, *J* = 6.9 Hz, 2H), 7.17 (d, *J* = 7.5 Hz, 2H), 7.08 (d, *J* = 8.0 Hz), 3.95 (s, 2H), 3.02 (s, 1H); $^{13}C\{^1H\}$ NMR (100 MHz, $CDCl_3$): δ 145.8, 144.7, 141.9, 140.5, 138.6, 138.2, 132.3, 131.5, 131.3, 129.0, 128.7, 128.0, 127.2, 126.9, 126.1, 119.8, 83.6, 77.2, 76.8, 64.1, 41.3; IR (ATR): 1506, 1484 cm^{-1}; HRMS (ESI): calcd for $C_{52}H_{39}$ ($[M + H]^+$), 663.3046; found, 663.3035.

*4-[Tris([1,1′-biphenyl]-4-yl)methyl]-N-methylaniline (**11**).* A mixture of tris([1,1′-biphenyl]-4-yl)methanol (2.44 g, 5.0 mmol) and *N*-methylaniline hydrochloride (1.44 g, 10 mmol, 2 equiv) in dry toluene (10 mL) and acetic acid (10 mL) was refluxed under Ar for 3 h. The mixture was cooled to rt and extracted with $CHCl_3$ (3 × 100 mL). Saturated $NaHCO_3$ aq (100 mL) was added to the combined organic layer, and the mixture was stirred for 1 h. The organic layer was separated, and the water layer was extracted with $CHCl_3$ (3 × 50 mL). The combined organic layer was dried over Na_2SO_4 and concentrated in vacuo. The residue was purified by silica gel column chromatography (hexane/$CHCl_3$ = 1/2) to yield **11** (608 mg, 1.1 mmol, 21%) as a white solid; mp 230.5−233.1 °C; ^{1}H NMR (500 MHz, $CDCl_3$): δ 7.59 (d, *J* = 8.0 Hz, 6H), 7.50 (d, *J* = 8.6 Hz, 6H), 7.40 (t, *J* = 8.0 Hz, 6H), 7.35 (d, *J* = 8.0 Hz, 6H), 7.30 (t, *J* = 7.5 Hz,

https://doi.org/10.1021/acs.joc.2c00086
J. Org. Chem. 2022, 87, 5744−5759

3H), 7.11 (d, J = 8.6 Hz, 2H), 6.58 (d, J = 8.0 Hz, 2H), 4.07 (br, 1H), 2.83 (s, 3H); $^{13}C\{^1H\}$ NMR (100 MHz, $CDCl_3$): δ 147.1, 146.4, 140.7, 138.3, 135.4, 132.0, 131.5, 128.7, 127.1, 126.9, 126.0, 111.5, 63.6, 30.7; IR (ATR): 1613, 1520, 1485, cm^{-1}; HRMS (ESI): calcd for $C_{44}H_{36}N$ ($[M + H]^+$), 578.2842; found, 578.2845.

General Procedure for Amination. A mixture of arylamine (1.0 equiv), ([4-iodophenyl]ethynyl)trimethylsilane **12** (1.1 equiv), NaO*t*-Bu in THF (1.0 M, 1.3 equiv), tri-*tert*-butylphosphonium tetrafluoroborate (10 mol %), $Pd_2(dba)_3$ (5 mol %), and toluene (4.0 mL/1.0 mmol of arylamine) was refluxed under Ar for 17 h. To the solution was added water, and the mixture was extracted with CH_2Cl_2. The combined organic layer was washed with water, dried over $MgSO_4$, and concentrated in vacuo. The residue was purified by column chromatography.

*4-[Tris([1,1′-biphenyl]-4-yl)methyl]-N,N-methyl-(4-[trimethylsilyl]ethynylphenyl)aniline (**13**).* Following the general procedure for amination, **11** (289 mg, 0.5 mmol), **12** (165 mg, 0.55 mmol, 1.1 equiv), NaO*t*-Bu in THF (1.0 M, 0.65 mL, 0.65 mmol, 1.3 equiv), tri-*tert*-butylphosphonium tetrafluoroborate (14.5 mg, 0.050 mmol), $Pd_2(dba)_3$ (22.9 mg, 0.025 mmol), and toluene (2.0 mL) were used. The residue was purified by silica gel column chromatography (hexane/CH_2Cl_2 = 2/1) to yield **13** (284 mg, 0.38 mmol, 76%) as a white solid; mp 224.0−225.7 °C; ^1H NMR (500 MHz, $CDCl_3$): δ 7.60 (d, J = 7.5 Hz, 6H), 7.53 (d, J = 8.6 Hz, 6H), 7.41 (t, J = 7.5 Hz, 6H), 7.36 (d, J = 8.6 Hz, 6H),7.30−7.33 (m, 5H), 7.23 (d, J = 6.9 Hz, 2H), 7.01 (d, J = 9.2 Hz, 2H), 6.87 (d, J = 8.6 Hz, 2H), 3.31 (s, 3H), 0.21 (s, 9H); $^{13}C\{^1H\}$ NMR (100 MHz, $CDCl_3$): δ 148.7, 145.9, 145.8, 141.1, 140.5, 138.6, 132.9, 132.0, 131.4, 128.7, 127.2, 126.9, 126.2, 121.5, 117.5, 113.8, 105.8, 92.3, 77.2, 63.8, 40.0, 0.1; IR (ATR): 1505, 1484 cm^{-1}; HRMS (ESI): calcd for $C_{55}H_{48}NSi$ ($[M]^+$), 750.3551; found, 750.3541.

*4-[Tris([1,1′-biphenyl]-4-yl)methyl]-N-(4-[trimethylsilyl]-ethynylphenyl)aniline (**14**).* Following the general procedure for amination, 4-[tris([1,1′-biphenyl]-4-yl)methyl]aniline **5** (564 mg, 1.0 mmol), **12** (330 mg, 1.1 mmol, 1.1 equiv), NaO*t*-Bu in THF (1.0 M, 1.3 mL, 1.3 mmol, 1.3 equiv), tri-*tert*-butylphosphonium tetrafluoroborate (29.0 mg, 0.10 mmol), $Pd_2(dba)_3$ (45.8 mg, 0.050 mmol), and toluene (4.0 mL) were used. The residue was purified by silica gel column chromatography (hexane/CH_2Cl_2 = 1/1) to yield **14** (437 mg, 0.594 mmol, 59%) as a white solid; mp 146.3−150.1 °C; ^1H NMR (500 MHz, $CDCl_3$): δ 7.60 (d, J = 7.5 Hz, 6H), 7.52 (d, J = 8.6 Hz, 6H), 7.41 (t, J = 7.5 Hz, 6H), 7.30−7.36 (m, 11H), 7.21 (d, J = 8.6 Hz, 2H), 7.02 (d, J = 8.6 Hz, 2H), 6.96 (d, J = 8.6 Hz, 2H), 5.81 (s, 1H), 0.21 (s, 9H); $^{13}C\{^1H\}$ NMR (126 MHz, $CDCl_3$): δ 145.9, 143.3, 140.5, 140.0, 139.7, 138.6, 133.2, 132.1, 131.4, 128.7, 127.2, 126.9, 126.1, 117.5, 116.2, 114.4, 92.3, 77.2, 63.8, 0.1; IR (ATR): 1600, 1514, 1486 cm^{-1}; HRMS (ESI): calcd for $C_{54}H_{46}NSi$ ($[M + H]^+$), 736.3394; found, 736.3409.

*4-[Tris([1,1′-biphenyl]-4-yl)methyl]-N,N-methyl-(4-ethynylphenyl)aniline (**3d**).* A mixture of **13** (298 mg 0.40 mmol), KOH (33.4 mg, 0.60 mmol, 1.5 equiv), MeOH (3.2 mL), and THF (12.8 mL) was stirred at rt for 1 h. To the solution was added water, and the mixture was extracted with EtOAc (3 × 20 mL). The combined organic layer was washed with brine, dried over Na_2SO_4, and concentrated in vacuo. The residue was purified by silica gel column chromatography (hexane/CH_2Cl_2 = 1/1) to yield **3d** (167 mg, 0.25 mmol, 63%) as a white solid; mp 217.1−219.0 °C; ^1H NMR (500 MHz, $CDCl_3$): δ 7.60 (d, J = 8.0 Hz, 6H), 7.53 (d, J = 8.0 Hz, 6H), 7.41 (t, J = 7.5 Hz, 6H), 7.30−7.37 (m, 11H), 7.25 (d, J = 5.2 Hz, 2H), 7.03 (d, J = 8.0 Hz, 2H), 6.88 (d, J = 8.0 Hz, 2H), 3.32 (s, 3H), 3.00 (s, 1H); $^{13}C\{^1H\}$ NMR (126 MHz, $CDCl_3$): δ 148.9, 145.9, 145.7, 141.3, 140.5, 138.6, 133.1, 132.1, 131.5, 128.7, 127.2, 126.9, 126.2, 121.7, 117.3, 112.5, 84.3, 75.6, 63.9, 40.0; IR (ATR): 1598, 1505, 1485 cm^{-1}; HRMS (ESI): calcd for $C_{52}H_{40}N$ ($[M + H]^+$), 678.3147; found, 678.3155.

*4-[Tris([1,1′-biphenyl]-4-yl)methyl]-N-(4-ethynylphenyl)aniline (**3f**).* A mixture of **14** (107 mg 0.15 mmol), KOH (12 mg, 0.22 mmol, 1.5 equiv), MeOH (1.6 mL), and THF (6.4 mL) was stirred at rt for 1 h. To the solution was added water, and the mixture was extracted with EtOAc (3 × 10 mL). The combined organic layer was washed with brine, dried over Na_2SO_4, and concentrated in vacuo. The residue was purified by silica gel column chromatography (hexane/CH_2Cl_2 = 1/1) to yield **3f** (87.0 mg, 0.073 mmol, 90%) as a white solid; mp 253.3−255.6 °C; ^1H NMR (500 MHz, $CDCl_3$): δ 7.60 (d, J = 7.5 Hz, 6H), 7.53 (d, J = 8.6 Hz, 6H), 7.42 (t, J = 7.5 Hz, 6H), 7.36 (d, J = 8.6 Hz, 6H), 7.36 (d, J = 8.6 Hz, 2H), 7.32 (t, J = 7.5 Hz, 3H), 7.23 (d, J = 8.6 Hz, 2H), 7.03 (d, J = 8.6 Hz, 2H), 6.98 (d, J = 8.6 Hz, 2H), 5.82 (s, 1H), 2.99 (s, 1H); $^{13}C\{^1H\}$ NMR (126 MHz, $CDCl_3$): δ 145.9, 143.7, 140.5, 140.2, 139.6, 138.6, 133.4, 132.1, 131.4, 128.7, 127.2, 126.9, 126.2, 117.7, 116.2, 113.3, 84.1, 75.7, 63.8; IR (ATR): 1600, 1510, 1485 cm^{-1}; HRMS (ESI): calcd for $C_{51}H_{38}N$ ($[M + H]^+$), 664.2999; found, 664.2996.

*N-([4-Tris([1,1′-biphenyl]-4-yl)methyl]phenyl)-4-ethynylbenzamide (**3h**).* A mixture of 4-[tris([1,1′-biphenyl]-4-yl)methyl]-benzenamine **5** (564 mg 1.0 mmol), 4-ethynylbenzoic acid **16** (146 mg, 1.0 mmol, 1.0 equiv), EDC (230 mg, 1.2 mmol, 1.2 equiv), and HOBt·H_2O (184 mg, 1.20 mmol, 1.2 equiv) in anhydrous dimethylformamide (DMF) (5 mL) was stirred at rt for 18 h. To the solution was added water, and the mixture was extracted with EtOAc (3 × 20 mL). The combined organic layer was washed with brine, dried over Na_2SO_4, and concentrated in vacuo. The residue was purified by silica gel column chromatography (hexane/CH_2Cl_2 = 1/2) to yield **3h** (600 mg, 0.87 mmol, 87%) as a white solid; mp 238.2−240.2 °C; ^1H NMR (500 MHz, $CDCl_3$): δ 7.81 (d, J = 8.0 Hz, 2H), 7.75 (s, 1H), 7.58−7.60 (m, 8H), 7.56 (d, J = 9.2 Hz, 2H), 7.52 (d, J = 8.6 Hz, 6H), 7.41 (t, J = 7.5 Hz, 6H), 7.30−7.37 (m, 11H), 3.21 (s, 1H); $^{13}C\{^1H\}$ NMR (126 MHz, $CDCl_3$): δ 164.9, 145.7, 143.2, 140.5, 138.7, 135.6, 134.8, 132.5, 131.8, 131.4, 128.7, 127.2, 127.0, 126.7, 126.2, 125.8, 119.4, 82.6, 79.9, 64.0; IR (ATR): 1673, 1597, 1518, 1487 cm^{-1}; HRMS (ESI): calcd for $C_{52}H_{38}NO$ ($[M + H]^+$), 692.2948; found, 692.2954.

*4-[Tris([1,1′-biphenyl]-4-yl)methyl]-N-(4-ethynylbenzyl)aniline (**3g**).* To a solution of **3h** (257 mg, 0.37 mmol) in anhydrous THF (5 mL) was added a suspension of $LiAlH_4$ (42.3 mg, 1.1 mmol, 3.0 equiv) in THF (1.1 mL) at 0 °C under Ar with stirring. The mixture was stirred at 70 °C for 2 h. To the mixture was added aqueous NaOH (7.5%, 0.2 mL), and the mixture was stirred for 5 min at rt. The mixture was filtered over Celite, and the filter cake was rinsed with EtOAc. The combined organic layer was dried over $MgSO_4$ and concentrated in vacuo. The residue was purified by silica gel column chromatography (hexane/CH_2Cl_2 = 1/1) to yield **3g** (227 mg, 0.335 mmol, 90%) as a white solid; mp 118.9−120.0 °C; ^1H NMR (500 MHz, $CDCl_3$): δ 7.59 (d, J = 8.0 Hz, 6H), 7.49 (d, J = 8.0 Hz, 6H), 7.45 (d, J = 8.0 Hz, 2H), 7.41 (t, J = 7.5 Hz, 6H), 7.29−7.34 (m, 11H), 7.09 (d, J = 8.6 Hz, 2H), 6.56 (d, J = 7.5 Hz, 2H), 4.31, (s, 2H), 4.08 (br, 1H) 3.04 (s, 1H); $^{13}C\{^1H\}$ NMR (100 MHz, $CDCl_3$): δ 146.3, 145.8, 140.6, 140.4, 138.4, 135.9, 132.4, 132.0, 131.5, 128.7, 127.4, 127.1, 126.9, 126.0, 120.9, 111.9, 83.5, 77.1, 63.6, 48.2; IR (ATR): 3425, 3286, 1611, 1514, 1485 cm^{-1}; HRMS (ESI): calcd for $C_{52}H_{40}N$ ($[M + H]^+$), 678.3155; found, 678.3152.

*4-[Tris([1,1′-biphenyl]-4-yl)methyl]-N,N-(4-ethynylbenzyl)-[(9H-fluoren-9-ylmethoxy)carbonyl]aniline (**3e**).* A mixture of **3g** (482 mg, 0.71 mmol), (9*H*-fluoren-9-yl)methyl carbonochloridate (221 mg, 0.85 mmol, 1.2 equiv) in dry $CHCl_3$ (10 mL) was stirred at 80 °C under Ar for 16 h. The solution was concentrated in vacuo. The residue was purified by silica gel column chromatography (hexane/CH_2Cl_2 = 1/1) to yield **3e** (583 mg, 0.65 mmol, 91%) as a white solid; mp 122.8−124.2 °C; ^1H NMR (400 MHz, $CDCl_3$, 333 K): δ 7.66 (d, J = 7.3 Hz, 2H), 7.60 (d, J = 7.8 Hz, 6H), 7.52 (d, J = 8.2 Hz, 6H), 7.41 (t, J = 7.3 Hz, 6H), 7.30−7.38 (m, 15H), 7.22 (dd, J = 7.3, 1.8 Hz, 2H), 7.17 (t, J = 7.3 Hz, 2H), 7.07 (d, J = 7.8 Hz, 2H), 6.93 (d, J = 7.8 Hz, 2H), 4.79 (s, 2H), 4.54 (d, J = 6.4 Hz, 2H), 4.11 (t, J = 6.4 Hz, 1H), 3.03 (s, J = 7.3 Hz, 1H); $^{13}C\{^1H\}$ NMR (126 MHz, $CDCl_3$): δ 155.5, 145.5, 145.1, 143.7, 141.3, 140.4, 139.3, 138.7, 138.5, 132.2, 131.6, 131.4, 128.7, 128.5, 127.6, 127.2, 126.9, 126.9, 126.2, 124.9, 121.0, 119.8, 83.4, 77.3, 67.4, 63.9, 53.9, 47.2; IR (ATR): 1716, 1512, 1488 cm^{-1}; HRMS (ESI): calcd for $C_{67}H_{50}NO_2$ ($[M + H]^+$), 900.3836; found, 900.3833.

*1-Azido-4-[tris([1,1′-biphenyl]-4-yl)methyl]benzene (**16**).* A mixture of **6** (1.08 g 1.6 mmol), NaN_3 (125 mg, 1.9 mmol, 1.2 equiv), L-

https://doi.org/10.1021/acs.joc.2c00086
J. Org. Chem. 2022, 87, 5744−5759

proline (36.8 mg, 0.32 mmol, 0.2 equiv), NaOH (12.8 mg, 0.32 mmol, 0.2 equiv), and CuI (30.5 mg, 0.160 mmol, 0.1 equiv) in dry DMSO (6 mL) was stirred at 90 °C under Ar for 6 h. To the mixture was added water at rt, and the mixture was extracted with EtOAc (3 × 20 mL). The combined organic layer was washed with brine, dried over Na_2SO_4, and concentrated in vacuo. The residue was purified by silica gel column chromatography (hexane/CH_2Cl_2 = 1/1) to yield **16** (430 mg, 0.73 mmol, 46%) as a white solid; mp 174.9−177.0 °C; ^{1}H NMR (500 MHz, $CDCl_3$): δ 7.59 (d, J = 7.5 Hz, 6H), 7.52 (d, J = 8.6 Hz, 6H), 7.41 (t, J = 8.0 Hz, 2H), 7.30−7.34 (m, 11H), 7.08 (d, J = 8.6 Hz, 2H); ^{13}C{^{1}H} NMR (75 MHz, $CDCl_3$): δ 145.5, 143.6, 140.4, 138.8, 137.8, 132.5, 131.4, 128.8, 127.3, 126.9, 126.3, 118.2, 63.9; IR (ATR): 2118, 2082, 1600, 1504, 1487 cm^{-1}; HRMS (FAB): calcd for $C_{43}H_{31}N_3$ ([M]$^+$), 589.2518; found, 589.2508.

*1-([4-Tris([1,1′-biphenyl]-4-yl)methyl]phenyl)-4-(4-ethynylphenyl)-1H-1,2,3-triazole (**3i**).* A mixture of **16** (177 mg, 0.30 mmol), ([4-ethynylphenyl]ethynyl)trimethylsilane (71.4 mg, 0.36 mmol, 1.15 equiv), L-sodium ascorbate (11.9 mg, 0.060 mmol, 0.2 equiv), and $CuSO_4 \cdot 5H_2O$ (15.0 mg, 0.060 mmol, 0.2 equiv) in dry DMF (5 mL) was stirred at rt for 2 days. Saturated NH_4Cl aq (10 mL) was poured into the solution, and the mixture was extracted with EtOAc (3 × 15 mL). The combined organic layer was washed with brine, dried over Na_2SO_4, and concentrated in vacuo. The residue was treated with a solution of KOH (252 mg, 0.45 mmol, 1.5 equiv) in a mixture of THF (16 mL) and MeOH (4 mL), and the mixture was stirred at rt for 1 h. Water was added to the solution, and the mixture was extracted with CH_2Cl_2 (3 × 15 mL). The combined organic layer was washed with brine, dried over Na_2SO_4, and concentrated in vacuo. The residue was purified by silica gel column chromatography (hexane/CH_2Cl_2 = 1/1) to yield **3i** (184 mg, 0.26 mmol, 86%) as a white solid; mp 226.0−227.2 °C; ^{1}H NMR (500 MHz, $CDCl_3$): δ 8.18 (s, 1H), 7.86 (d, J = 8.6 Hz, 2H), 7.71 (d, J = 9.2 Hz, 2H), 7.60 (d, J = 8.6 Hz, 6H), 7.53−7.58 (m, 10H), 7.42 (t, J = 7.5 Hz, 6H), 7.38 (d, J = 8.6 Hz, 6H), 7.33 (t, J = 7.5 Hz, 3H), 3.13 (s, 1H); ^{13}C{^{1}H} NMR (126 MHz, $CDCl_3$): δ 147.9, 147.6, 145.2, 140.3, 139.0, 134.8, 132.7, 132.4, 131.3, 130.5, 128.8, 127.4, 127.0, 126.4, 125.6, 122.0, 119.8, 117.9, 83.4, 78.1, 64.2; IR (ATR): 3285, 1516, 1486 cm^{-1}; HRMS (FAB): calcd for $C_{53}H_{38}N_3$ ([M]$^+$), 716.3066; found, 716.3066.

General Procedure A for the Synthesis of [2]Rotaxanes. A mixture of macrocyclic phenanthroline−CuI complex **2** (1.0 equiv), alkyne (2.5 equiv), K_2CO_3 (10 equiv), and I_2 (1.0 equiv) in dry THF (6.25 mL/0.1 mmol of **2**) was stirred at 60 °C under Ar for 24 h. Then, K_2CO_3 (10 equiv) and I_2 (1.0 equiv) were added, and the mixture was stirred again at 60 °C for 24 h. The mixture was cooled to rt, and CH_2Cl_2 (7.5 mL/0.1 mmol of **2**), CH_3CN (17.5 mL/0.1 mmol of **2**), and NH_3 aq (30%, 8.5 mL/0.1 mmol of **2**) were added. After stirring at rt overnight, the solution was extracted with CH_2Cl_2, dried over Na_2SO_4, and concentrated in vacuo. The residue was purified by column chromatography and GPC.

General Procedure B for the Synthesis of [2]Rotaxanes. A mixture of macrocyclic phenanthroline−CuI complex **2** (1.0 equiv), alkyne (2.5 equiv), K_2CO_3 (3.75 equiv), and I_2 (1.25 equiv) in dry THF (6.25 mL/0.1 mmol of **2**) was stirred at 60 °C under Ar for 48 h. The solution was cooled to rt, and CH_2Cl_2 (7.5 mL/0.1 mmol of **2**), CH_3CN (17.5 mL/0.1 mmol of **2**), and NH_3 aq (30%, 8.5 mL/0.1 mmol of **2**) were added. After stirring at rt overnight, the solution was extracted with CH_2Cl_2. The organic layer was dried over Na_2SO_4 and concentrated in vacuo. The residue was purified by column chromatography and GPC.

*[2]Rotaxane (**4a**) and Diyne (**17a**).* Following the general procedure A, **2** (77.3 mg, 0.10 mmol), **3a** (143 mg, 0.25 mmol), K_2CO_3 (138 + 138 mg, 1.0 + 1.0 mmol), and I_2 (25.4 + 25.4 mg, 0.10 + 0.10 mmol) were used. The residue was purified by silica gel column chromatography (hexane/$CHCl_3$ = 1/1) to yield **4a** (108 mg, 0.063 mmol, 86%) as a white solid. The diyne **17a** (28 mg, 0.024 mmol, 20%, based on **3a**) was also isolated as a white solid. Data for **4a**: mp 182.1−184.9 °C; ^{1}H NMR (500 MHz, $CDCl_3$): δ 8.38 (d, J = 8.6 Hz, 4H), 8.14 (d, J = 8.6 Hz, 2H), 7.96 (d, J = 8.6 Hz, 2H), 7.62 (s, 2H), 7.53 (d, J = 8.6 Hz, 12H), 7.38−7.41 (m, 28H), 7.30 (t, J = 7.5 Hz, 6H), 7.20 (d, J = 8.6 Hz, 4H), 7.15 (d, J = 8.6 Hz, 12H), 7.04 (t, J = 8.0 Hz, 1H), 7.00 (d, J = 8.6 Hz, 4H), 6.98 (t, J = 2.3 Hz, 1H), 6.42 (dd, J = 2.3, 8.6 Hz, 2H), 4.22 (t, J = 7.5 Hz, 4H), 4.08 (t, J = 6.3 Hz, 4H), 2.05 (quint, J = 7.5 Hz, 4H), 1.91 (quint, J = 6.6 Hz, 4H); ^{13}C{^{1}H} NMR (126 MHz, $CDCl_3$): δ 160.4, 159.9, 156.3, 147.8, 146.1, 145.1, 140.4, 138.6, 136.4, 132.14, 132.08, 131.2, 130.7, 129.5, 129.2, 128.7, 127.2, 126.9, 126.2, 125.4, 119.0, 118.9, 115.1, 107.5, 101.8, 83.2, 75.1, 68.0, 67.7, 64.2, 26.2, 25.8; IR (ATR): 1601, 1586, 1485 cm^{-1}; HRMS (MALDI): calcd for $C_{128}H_{97}N_2O_4$ ([M + H]$^+$), 1425.7424; found, 1725.7443. Data for **17a**: mp 333.7−334.2 °C; ^{1}H NMR (500 MHz, $CDCl_3$): δ 7.59 (d, J = 8.0 Hz, 12H), 7.52 (d, J = 8.0 Hz, 12H), 7.45 (d, J = 8.6 Hz, 4H), 7.41 (t, J = 7.5 Hz, 12H), 7.30−7.33 (m, 22H); ^{13}C{^{1}H} NMR (126 MHz, $CDCl_3$): δ 148.1, 145.2, 140.4, 138.8, 131.8, 131.4, 131.1, 128.8, 127.3, 127.0, 126.3, 119.4, 81.5, 74.1, 64.4; IR (ATR): 1599, 1486 cm^{-1}; HRMS (MALDI): calcd for $C_{90}H_{63}$ ([M + H]$^+$), 1143.4924; found, 1143.4961.

*[2]Rotaxane (**4b**).* Following the general procedure A, **2** (77.3 mg, 0.10 mmol), **3b** (168 mg, 0.25 mmol), K_2CO_3 (138 + 138 mg, 1.0 + 1.0 mmol), and I_2 (25.4 + 25.4 mg, 0.10 + 0.10 mmol) were used. The residue was purified by silica gel column chromatography (hexane/$CHCl_3$ = 1/1) to yield **4b** (95 mg, 0.049 mmol, 49%) as a white solid; mp 191.8−195.9 °C; ^{1}H NMR (500 MHz, $CDCl_3$): δ 8.37 (d, J = 8.6 Hz, 4H), 8.22 (d, J = 8.0 Hz, 2H), 8.00 (d, J = 8.6 Hz, 2H), 7.72 (s, 2H), 7.57 (d, J = 6.9 Hz, 12H), 7.47 (d, J = 8.0 Hz, 12H), 7.44 (d, J = 8.6 Hz, 4H), 7.40 (t, J = 8.0 Hz, 12H), 7.37 (d, J = 8.6 Hz, 4H), 7.27−7.32 (m, 22H), 7.23 (d, J = 5.7 Hz, 4H), 7.16 (t, J = 8.0 Hz, 1H), 7.11 (d, J = 9.2 Hz, 4H), 7.02 (t, J = 2.3 Hz, 2H), 6.51 (dd, J = 2.3, 8.0 Hz, 2H), 4.10 (t, J = 7.5 Hz, 4H), 4.06 (t, J = 6.3 Hz, 4H), 1.99 (quint, J = 7.5 Hz, 4H), 1.88 (quint, J = 6.6 Hz, 4H); ^{13}C{^{1}H} NMR (126 MHz, $CDCl_3$): δ 160.4, 159.8, 156.5, 147.2, 146.2, 145.3, 140.3, 138.6, 136.4, 132.5, 132.2, 131.5, 131.3, 131.0, 129.8, 129.2, 128.7, 127.3, 127.2, 126.9, 126.2, 125.4, 124.0, 121.0, 120.4, 119.3, 115.0, 107.1, 102.2, 92.2, 89.4, 83.0, 76.1, 67.9, 67.7, 64.2, 26.2, 25.7; IR (ATR): 1601, 1587, 1485, cm^{-1}; HRMS (MALDI): calcd for $C_{144}H_{105}N_2O_4$ ([M + H]$^+$), 1925.8069; found, 1925.8129.

*[2]Rotaxane (**4c**) and Diyne (**17c**).* Following the general procedure A, **2** (15.5 mg, 0.020 mmol), **3c** (33.1 mg, 0.050 mmol), K_2CO_3 (28 + 28 mg, 0.20 + 0.20 mmol), and I_2 (5.1 + 5.1 mg, 0.020 + 0.020 mmol) were used. The residue was purified by silica gel column chromatography (hexane/$CHCl_3$ = 1/1) to yield **4c** (15 mg, 0.0077 mmol, 39%) as a white solid. The axle **17c** (8.7 mg, 0.0066 mmol, 26%, based on **3c**) was also isolated as a white solid. Data for **4c**: mp 181.3−184.2 °C; ^{1}H NMR (500 MHz, $CDCl_3$): δ 8.36 (d, J = 8.0 Hz, 4H), 8.15 (d, J = 8.6 Hz, 2H), 7.93 (d, J = 8.0 Hz, 2H), 7.68 (s, 2H), 7.57 (d, J = 8.0 Hz, 12H), 7.47 (d, J = 7.5 Hz, 12H), 7.40 (t, J = 7.5 Hz, 12H), 7.38 (d, J = 7.5 Hz, 4H), 7.29−7.32 (m, 18H), 7.14 (d, J = 8.6 Hz, 8H), 7.10 (t, J = 8.6 Hz, 1H), 7.00 (s, 1H), 6.91 (t, J = 6.9 Hz, 8H), 6.49 (d, J = 8.6 Hz, 2H), 4.16 (t, J = 8.0 Hz, 4H), 4.10 (t, J = 6.9 Hz, 4H), 3.77 (s, 4H), 2.02 (quint, J = 7.5 Hz, 4H), 1.91 (quint, J = 6.9 Hz, 4H); ^{13}C{^{1}H} NMR (126 MHz, $CDCl_3$): δ 160.5, 159.9, 156.4, 146.1, 145.8, 144.5, 142.1, 140.5, 138.5, 138.0, 136.4, 132.9, 132.1, 131.4, 131.1, 129.6, 129.1, 129.0, 128.7, 128.0, 127.2, 126.9, 126.1, 125.4, 119.1, 119.0, 115.0, 107.8, 101.7, 83.0, 74.7, 68.0, 67.7, 64.0, 41.2, 26.0, 25.9; IR (ATR): 1602, 1587, 1487 cm^{-1}; HRMS (MALDI): calcd for $C_{142}H_{109}N_2O_4$ ([M + H]$^+$), 1905.8382; found, 1905.8391. Data for **17c**: mp 289.7−291.2 °C; ^{1}H NMR (500 MHz, $CDCl_3$): δ 7.59 (d, J = 8.0 Hz, 12H), 7.50 (d, J = 7.5 Hz, 12H), 7.44 (t, J = 8.0 Hz, 4H), 7.40 (t, J = 6.9 Hz, 12H), 7.29−7.34 (m, 18H), 7.23 (d, J = 7.5 Hz, 4H), 7.18 (d, J = 7.5 Hz, 4H), 7.08 (d, J = 8.0 Hz, 4H), 3.96 (s, 4H); ^{13}C{^{1}H} NMR (126 MHz, $CDCl_3$): δ 145.8, 144.7, 142.5, 140.6, 138.6, 138.0, 132.6, 131.5, 131.3, 129.2, 128.7, 128.1, 127.2, 127.0, 126.1, 119.6, 81.5, 73.7, 64.1, 41.4; IR (ATR): 1487, 1427, 1411 cm^{-1}; HRMS (MALDI): calcd for $C_{104}H_{75}$ ([M + H]$^+$), 1323.5863; found, 1323.5844.

*[2]Rotaxane (**4d**) and Diyne (**17d**).* Following the general procedure A, **2** (15.5 mg, 0.020 mmol), **3d** (33.9 mg, 0.050 mmol), K_2CO_3 (28 + 28 mg, 0.20 + 0.20 mmol), and I_2 (5.1 + 5.1 mg, 0.020 + 0.020 mmol) were used. The residue was purified by silica gel column chromatography (hexane/$CHCl_3$ = 1/1) to yield **4d** (11 mg,

https://doi.org/10.1021/acs.joc.2c00086
J. Org. Chem. 2022, 87, 5744−5759

0.0057 mmol, 28%) as a brown solid. The axle **17d** (16.2 mg, 0.012 mmol, 48% based on **3d**) was also isolated as a yellow solid. Data for **4d**: mp 199.8−201.0 °C; ^{1}H NMR (500 MHz, $CDCl_3$): δ 8.48 (d, J = 9.2 Hz, 4H), 8.14 (d, J = 8.6 Hz, 2H), 7.98 (d, J = 8.6 Hz, 2H), 7.65 (s, 2H), 7.59 (d, J = 7.5 Hz, 12H), 7.50 (d, J = 8.6 Hz, 12H), 7.41 (t, J = 7.5 Hz, 12H), 7.30−7.32 (m, 22H), 7.25 (d, J = 6.9 Hz, 4H), 7.15 (d, J = 8.6 Hz, 4H), 7.12 (t, J = 8.0 Hz, 1H), 7.06 (1H, s), 6.88 (d, J = 8.6 Hz, 4H), 6.61 (d, J = 8.6 Hz, 4H), 6.51 (dd, J = 2.3, 8.6 Hz, 2H), 4.23 (t, J = 8.0 Hz, 4H), 4.18 (t, J = 6.9 Hz, 4H), 3.17 (s, 6H), 2.06 (quint, J = 7.5 Hz, 4H), 1.96 (quint, J = 6.9 Hz, 4H); ^{13}C{^{1}H} NMR (126 MHz, $CDCl_3$): δ 160.6, 160.1, 156.1, 148.8, 146.0, 145.8, 145.3, 141.5, 140.5, 138.5, 136.3, 133.6, 132.0, 131.9, 131.4, 129.5, 129.1, 128.7, 127.2, 127.1, 126.9, 126.1, 125.3, 122.0, 118.7, 116.8, 115.1, 111.5, 108.3, 101.3, 83.7, 74.3, 68.1, 67.8, 63.8, 39.8, 26.0, 25.9; IR (ATR): 1590, 1505, 1485 cm^{-1}; HRMS (MALDI): calcd for $C_{142}H_{111}N_4O_4$ ([M + H]$^+$), 1935.8600; found, 1935.8669. Data for **17d**: mp 250.9−252.0 °C; ^{1}H NMR (500 MHz, $CDCl_3$): δ 7.60 (d, J = 7.5 Hz, 12H), 7.53 (d, J = 8.0 Hz, 12H), 7.41 (t, J = 7.5 Hz, 12H), 7.35−7.37 (m, 16H), 7.31 (t, J = 7.5 Hz, 6H), 7.27 (d, J = 8.6 Hz, 4H), 7.06 (d, J = 8.6 Hz, 4H), 6.84 (d, J = 8.6 Hz, 4H), 3.33 (s, 6H); ^{13}C{^{1}H} NMR (126 MHz, $CDCl_3$): δ 149.1, 145.8, 145.5, 142.0, 140.5, 138.6, 133.5, 132.2, 131.5, 128.8, 127.2, 127.0, 126.2, 122.6, 116.6, 111.8, 82.1, 73.1, 63.9, 40.1; IR (ATR): 1595, 1504, 1487 cm^{-1}; HRMS (MALDI): calcd for $C_{104}H_{76}N_2$ ([M]$^+$), 1352.6003; found, 1352.5990.

*[2]Rotaxane (**4e**).* A mixture of **2** (77.3 mg, 0.10 mmol), **3e** (225 mg, 0.25 mmol 2.5 equiv), K_2CO_3 (51.8 mg, 0.375 mmol, 3.75 equiv), and I_2 (31.7 mg, 0.125 mmol, 1.25 equiv) in dry THF (6.25 mL) was stirred at 60 °C under Ar for 48 h. The mixture was cooled to rt, and CH_2Cl_2 (17.5 mL), CH_3CN (17.5 mL), KCN (52.1 mg, 0.80 mmol, 8.0 equiv), and water (10 mL) were added. After stirring at rt for 1 h, the mixture was extracted with CH_2Cl_2, dried over Na_2SO_4, and concentrated in vacuo. The residue was purified by silica gel column chromatography (hexane/AcOEt = 2/1) and GPC to yield **4e** (112 mg, 0.047 mmol, 47%) as a white solid; mp 158.7−160.1 °C; ^{1}H NMR (500 MHz, $CDCl_3$): δ 8.39 (d, J = 7.5 Hz, 4H), 8.05 (d, J = 6.9 Hz, 2H), 7.69 (d, J = 8.6 Hz, 2H), 7.58−7.60 (m, 18H), 7.50 (d, J = 6.9 Hz, 12H), 7.40−7.44 (m, 16H), 7.29−7.34 (m, 18H), 7.23−7.25 (m, 8H), 7.15−7.17 (m, 8H), 7.09−7.11 (m, 5H), 7.05 (s, 1H), 6.79 (br, 8H), 6.49 (d, J = 8.0 Hz, 2H), 4.60 (s, 4H), 4.23 (d, J = 5.2 Hz, 4H), 4.15 (t, J = 7.5 Hz, 4H), 4.10 (t, J = 6.3 Hz, 4H), 3.98 (t, J = 5.7 Hz, 2H), 2.01 (quint, J = 6.9 Hz, 4H), 1.88 (quint, J = 6.3 Hz, 4H); ^{13}C{^{1}H} NMR (126 MHz, $CDCl_3$): δ 160.4, 159.9, 156.2, 155.4, 146.0, 145.5, 144.9, 143.6, 141.2, 140.4, 139.5, 139.1, 138.6, 136.4, 132.9, 131.9, 131.5, 131.4, 129.6, 129.1, 128.7, 128.5, 127.5, 127.2, 127.2, 126.9, 126.6, 126.2, 125.9, 125.3, 124.8, 120.2, 119.8, 118.9, 115.0, 107.6, 101.8, 83.0, 75.0, 68.0, 67.7, 67.2, 63.9, 53.8, 47.1, 26.1, 25.8; IR (ATR): 1716, 1605, 1489 cm^{-1}; HRMS (MALDI): calcd for $C_{172}H_{131}N_4O_8$ ([M + H]$^+$), 2379.9961; found, 2379.9975.

*[2]Rotaxane (**4f**) and Diyne (**17f**).* Following the general procedure A, **2** (40.2 mg, 0.052 mmol), **3f** (86.3 mg, 0.13 mmol), K_2CO_3 (72 + 72 mg, 0.052 + 0.052 mmol), and I_2 (13 + 13 mg, 0.52 + 0.52 mmol) were used. The residue was purified by silica gel column chromatography (hexane/$CHCl_3$ = 1/2) to yield **4f** (32 mg, 0.012 mmol, 24%) as a brown solid. The axle **17f** (41 mg, 0.031 mmol, 48%, based on **3f**) was also isolated as a brown solid. Data for **4f**: mp 206.3−208.0 °C. ^{1}H NMR (500 MHz, $CDCl_3$): δ 8.26 (d, J = 8.0 Hz, 2H), 7.84 (d, J = 8.6 Hz, 2H), 7.78 (s, 2H), 7.68 (s, 2H), 7.61 (d, J = 8.6 Hz, 4H), 7.58 (d, J = 7.5 Hz, 12H), 7.48 (d, J = 8.6 Hz, 12H), 7.40 (t, J = 7.5 Hz, 12H), 7.29−7.32 (m, 18H), 7.19 (d, J = 8.6 Hz, 4H), 7.02−7.05 (m, 5H), 6.93 (d, J = 8.6 Hz, 4H), 6.87 (d, J = 8.6 Hz, 4H), 6.58−6.60 (m, 5H), 6.39 (dd, J = 2.3, 8.0 Hz, 2H), 3.92 (t, J = 6.3 Hz, 4H), 3.84 (t, J = 6.9 Hz, 4H), 1.75−1.81 (m, 8H); ^{13}C{^{1}H} NMR (126 MHz, $CDCl_3$): δ 160.3, 159.3, 159.2, 146.5, 146.1, 144.2, 140.6, 139.8, 138.9, 138.5, 136.6, 133.4, 132.7, 131.6, 131.5, 130.0, 129.8, 128.7, 128.5, 127.5, 127.2, 126.9, 126.0, 125.8, 121.9, 117.3, 115.5, 114.1, 111.4, 106.8, 101.8, 82.5, 72.9, 67.3, 63.7, 25.8, 25.4; IR (ATR): 3398, 1596, 1512, 1486 cm^{-1}; HRMS (MALDI): calcd for $C_{140}H_{107}N_4O_4$ ([M + H]$^+$), 1907.8287; found, 1907.8234. Data for **17f**: mp 272.4−274.2 °C; ^{1}H NMR (500 MHz, $CDCl_3$): δ 7.60 (d, J = 7.5 Hz, 12H), 7.52 (d, J = 8.0 Hz, 12H), 7.41 (t, J = 7.5 Hz, 12H), 7.35−7.38 (m, 16H), 7.31 (t, J = 8.0 Hz, 6H), 7.23 (d, J = 8.0 Hz, 4H), 7.04 (d, J = 8.6 Hz, 4H), 6.97 (d, J = 8.6 Hz, 4H), 5.87 (s, 2H); ^{13}C NMR (126 MHz, $CDCl_3$): δ 145.9, 144.0, 140.5, 139.3, 138.6, 133.8, 132.1, 131.4, 128.7, 127.2, 126.9, 126.2, 118.0, 116.0, 112.9, 81.9, 73.1, 63.8; IR (ATR): 3398, 1595, 1505, 1484, cm^{-1}; HRMS (MALDI): calcd for $C_{102}H_{73}N_2$ ([M]$^+$), 1324.5690; found, 1324.5662.

The synthesis of **4f** was also studied by following procedure B. Compound **2** (86 mg, 0.11 mmol), **3f** (184 mg, 0.28 mmol), K_2CO_3 (57 mg, 0.42 mmol), and I_2 (35 mg, 0.14 mmol) were used. The residue was purified by silica gel column chromatography (hexane/$CHCl_3$ = 1/2) to yield **4f** (126 mg, 0.066 mmol, 60%) as a brown solid.

*[2]Rotaxane (**4g**) and Diyne (**17g**).* Following the general procedure A, **2** (15.5 mg, 0.020 mmol), **3g** (33.9 mg, 0.050 mmol), K_2CO_3 (28 + 28 mg, 0.20 + 0.20 mmol), and I_2 (5.1 + 5.1 mg, 0.020 + 0.020 mmol) were used. The residue was purified by silica gel column chromatography (hexane/$CHCl_3$ = 1/1) to yield **4g** (2.5 mg, 0.0020 mmol, 6.4%) as a brown solid. The axle **17g** (14 mg, 0.010 mmol, 41% based on **3g**) was also isolated as a white solid. Data for **4g**: mp 187.9−188.6 °C; ^{1}H NMR (500 MHz, $CDCl_3$): δ 8.24 (d, J = 8.0 Hz, 2H), 8.03 (d, J = 7.5 Hz, 4H), 7.92 (d, J = 8.6 Hz, 2H), 7.75 (s, 2H), 7.58 (d, J = 8.0 Hz, 12H), 7.48 (d, J = 7.5 Hz, 12H), 7.40 (t, J = 6.9 Hz, 12H), 7.30−7.33 (m, 18H), 7.02 (d, J = 8.2 Hz, 4H), 6.98 (d, J = 8.0 Hz, 5H), 6.79 (d, J = 8.0 Hz, 4H), 6.55 (d, J = 8.6 Hz, 4H), 6.35 (d, J = 7.5 Hz, 3H), 5.11 (s, 2H), 3.95 (t, J = 6.3 Hz, 4H), 3.90 (s, 4H), 3.70 (t, J = 5.7 Hz, 4H), 1.76 (m, 8H); ^{13}C{^{1}H} NMR (126 MHz, $CDCl_3$): δ 160.3, 159.6, 158.4, 146.7, 146.61, 146.55, 141.7, 140.8, 138.5, 136.7, 135.1, 133.0, 132.8, 131.9, 131.6, 130.3, 129.7, 128.9, 127.6, 127.4, 127.3, 127.1, 126.1, 125.9, 120.9, 120.1, 114.7, 112.2, 107.5, 100.9, 82.2, 74.2, 67.5, 67.4, 63.7, 48.1, 25.8, 25.5; IR (ATR): 3420, 3331, 1605, 1586, 1515, 1487 cm^{-1}; HRMS (MALDI): calcd for $C_{142}H_{111}N_4O_4$ ([M + H]$^+$), 1935.8600; found, 1935.8665. Data for **17g**: mp 249.7−250.9 °C;^{1}H NMR (500 MHz, $CDCl_3$): δ 7.59 (d, J = 8.0 Hz, 12H), 7.50−7.47 (m, 16H), 7.40 (t, J = 7.5 Hz, 12H), 7.34−7.29 (m, 22H), 7.08 (d, J = 8.6 Hz, 4H), 6.54 (d, J = 8.6 Hz, 4H), 4.33 (s, 4H), 4.08 (br, 2H); ^{13}C{^{1}H} NMR (100 MHz, $CDCl_3$): δ 146.3, 145.8, 140.6, 140.4, 138.3, 135.9, 132.6, 132.4, 132.0, 131.5, 128.7, 127.3, 127.1, 126.9, 126.0, 122.2, 111.9, 93.9, 63.6, 48.2; IR (ATR): 3412, 1608, 1513, 1485 cm^{-1}; HRMS (MALDI): calcd for $C_{104}H_{77}N_2$ ([M + H]$^+$), 1353.6081; found, 1353.6067.

*[2]Rotaxane (**4h**) and Diyne (**17h**).* Following the general procedure A, **2** (77.3 mg, 0.10 mmol), **3h** (173 mg, 0.25 mmol), K_2CO_3 (138 + 138 mg, 1.0 + 1.0 mmol), and I_2 (25.4 + 25.4 mg, 0.10 + 0.10 mmol) were used. The residue was purified by silica gel column chromatography (hexane/$CHCl_3$ = 1/2) to yield **4h** (91 mg, 0.046 mmol, 46%) as a yellow solid. The axle **17h** (42 mg, 0.030 mmol, 80%, based on **3h**) was also isolated as a white solid. Data for **4h**: mp 214.2−216.6 °C; ^{1}H NMR (500 MHz, $CDCl_3$): δ 9.42 (s, 2H), 8.27 (d, J = 8.6 Hz, 2H), 7.97 (d, J = 8.0 Hz, 4H), 7.82 (s, 2H), 7.72 (d, J = 8.0 Hz, 2H), 7.58 (d, J = 8.0 Hz, 12H), 7.48−7.51 (m, 16H), 7.40 (t, J = 8.0 Hz, 12H), 7.27−7.35 (m, 26H), 7.10 (d, J = 8.6 Hz, 4H), 7.06 (t, J = 8.6 Hz, 1H), 6.93 (s, 1H), 6.57 (d, J = 8.6 Hz, 4H), 6.43 (dd, J = 2.3, 8.0 Hz, 2H), 4.04 (t, J = 5.7 Hz, 4H), 3.98 (t, J = 6.3 Hz, 4H), 1.83−1.87 (m, 8H); ^{13}C{^{1}H} NMR (126 MHz, $CDCl_3$): δ 164.4, 160.5, 159.5, 159.1, 146.1, 145.9, 142.1, 140.5, 138.5, 136.6, 136.3, 135.3, 132.5, 132.0, 131.4, 131.1, 129.6, 129.5, 128.7, 127.6, 127.5, 127.2, 126.9, 126.1, 125.9, 124.2, 122.1, 119.6, 114.2, 107.3, 100.9, 81.8, 75.5, 67.3, 67.2, 63.9, 25.5, 25.3; IR (ATR): 1667, 1601, 1511, 1486 cm^{-1}; HRMS (MALDI): calcd for $C_{142}H_{107}N_4O_6$ ([M + H]$^+$), 1963.8185; found, 1963.8180. Data for **17h**: mp 260.6−262.6 °C;^{1}H NMR (500 MHz, $CDCl_3$): δ 7.83 (d, J = 8.6 Hz, 4H), 7.78 (s, 2H), 7.61 (d, J = 8.6 Hz, 4H), 7.60 (d, J = 8.0 Hz, 12H), 7.52 (d, J = 8.0 Hz, 12H), 7.41 (t, J = 7.5 Hz, 12H), 7.30−7.37 (m, 22H); ^{13}C{^{1}H} NMR (126 MHz, $CDCl_3$): δ 164.7, 145.7, 143.3, 140.5, 138.7, 135.5, 135.3, 132.9, 131.8, 131.4, 128.7, 127.2, 127.1, 127.0, 126.3, 125.1, 119.4, 81.6, 76.1, 64.0; IR (ATR): 3439,

https://doi.org/10.1021/acs.joc.2c00086
J. Org. Chem. 2022, 87, 5744−5759

1682, 1600, 1519, 1487 cm^{-1}; HRMS (MALDI): calcd for $C_{104}H_{73}N_2O_2$ ($[M + H]^+$), 1381.5667; found, 1381.5610.

*[2]Rotaxane (**4i**) and Diyne (**17i**).* Following the general procedure A, **2** (77.3 mg, 0.10 mmol), **3i** (179 mg, 0.25 mmol), K_2CO_3 (138 + 138 mg, 1.0 + 1.0 mmol), and I_2 (25.4 + 25.4 mg, 0.10 + 0.10 mmol) were used. The residue was purified by silica gel column chromatography (hexane/$CHCl_3$ = 1/2) to yield **4i** (98 mg, 0.048 mmol, 48%) as a white solid. The axle **17i** (62 mg, 0.043 mmol, 35% based on **3i**) was also isolated as a yellow solid. Data for **4i**: mp 219.2−225.7 °C; ^{1}H NMR (500 MHz, $CDCl_3$): δ 9.34 (s, 2H), 8.25 (d, J = 8.0 Hz, 2H), 7.91 (d, J = 8.0 Hz, 4H), 7.80 (s, 2H), 7.72−7.77 (m, 10H), 7.59 (d, J = 7.5 Hz, 12H), 7.52 (d, J = 8.6 Hz, 12H), 7.41 (t, J = 8.0 Hz, 12H), 7.30−7.36 (m, 26H), 7.16 (t, J = 2.3 Hz, 1H), 7.07 (t, J = 8.6 Hz, 1H), 6.48 (dd, J = 2.3, 8.6 Hz, 2H), 6.38 (d, J = 8.6 Hz, 4H), 4.14 (t, J = 6.3 Hz, 4H), 3.84 (t, J = 6.9 Hz, 4H), 1.84 (quint, J = 7.5 Hz, 4H), 1.77 (quint, J = 6.9 Hz, 4H); ^{13}C{^{1}H} NMR (126 MHz, $CDCl_3$): δ 160.6, 159.2, 159.1, 147.0, 146.9, 146.7, 145.3, 140.4, 138.8, 136.5, 134.7, 133.0, 132.7, 131.8, 131.35, 131.28, 129.5, 129.4, 128.8, 127.4, 127.3, 126.9, 126.4, 125.8, 125.5, 121.5, 120.8, 120.5, 119.3, 114.1, 108.0, 100.6, 82.1, 74.6, 67.3, 67.1, 64.1, 25.24, 25.22; IR (ATR): 1601, 1586, 1516, 1483 cm^{-1}; HRMS (MALDI): calcd for $C_{144}H_{107}N_8O_4$ ($[M + H]^+$), 2011.8410; found, 2011.8481. Data for **17i**: mp 234.5−236.8 °C; ^{1}H NMR (500 MHz, $CDCl_3$): δ 8.19 (s, 2H), 7.88 (d, J = 6.9 Hz, 4H), 7.71 (d, J = 7.5 Hz, 4H), 7.61−7.60 (m, 16H), 7.56−7.53 (m, 16H), 7.42 (t, J = 7.5 Hz, 12H), 7.38 (d, J = 7.5 Hz, 12H), 7.33 (t, J = 7.5 Hz, 6H); ^{13}C{^{1}H} NMR (100 MHz, $CDCl_3$): δ 148.0, 147.5, 145.2, 140.4, 139.0, 134.8, 133.1, 132.5, 131.4, 131.0, 128.8, 127.4, 127.0, 126.4, 125.7, 119.8, 118.0, 74.9, 64.2 (two signals are missing); IR (ATR): 1600, 1515, 1485 cm^{-1}; HRMS (MALDI): calcd for $C_{106}H_{73}N_6$ ($[M + H]^+$), 1429.5891; found, 1429.5851.

Synthesis of 4g by the Removal of the Fmoc Group from 4e. A solution of **4e** (72 mg, 0.030 mmol) in diethylamine (0.10 mL), acetonitrile (2.0 mL), and dichloromethane (8.0 mL) was stirred at rt under Ar for 4 h. To the mixture was added water, and the mixture was extracted with CH_2Cl_2 (3 × 3 mL). The combined organic layer was washed with brine, dried over Na_2SO_4, and concentrated in vacuo. The residue was purified by silica gel column chromatography (hexane/AcOEt = 1/1) and GPC to yield **4g** (49 mg, 0.025 mmol, 84%) as a white solid.

Preparation and Observation of the ^{1}H NMR Spectrum of 4f-d_2. A solution of **4f** (27 mg, 0.014 mmol) in CH_3OD (99 atom % D, 1.2 mL) and anhydrous dichloromethane (1.2 mL) was stirred at rt under Ar overnight. Volatiles were removed under reduced pressure to yield the desired deuterated compound, **4f-d_2** (26 mg, 0.014 mmol, quint, 78 atom % D of the N−D bond, estimated by ^{1}H NMR in $CDCl_3$) as a light yellow solid.

In order to reduce the deuteration loss due to water and possible residual acidic impurities in the solvent used for recording NMR, it was imperative to include a simple pre-treatment for these solvents. NMR solvents ($CDCl_3$ for confirming deuteration and deuterated toluene-d_8 for VT NMR experiments) were thoroughly washed with equal volume of D_2O followed by drying over sodium sulfate before use.

X-ray Diffraction Studies. A suitable single crystal was selected in Fomblin Y perfluoropolyether (HVAC 140/13) at ambient temperature. All diffraction data were collected at −173 °C on a Bruker Apex II Ultra X-ray diffractometer equipped with a Mo Kα radiation (λ = 0.71073 Å) source. Intensity data were processed using the Apex3 software suite. The solution of the structures and the corresponding refinements were carried out using the Yadokari-XG[31] graphical interface. The positions of the non-hydrogen atoms were determined by using the SHELXT-2014/5 and 2018/2[32] program and refined on F^2 by the full-matrix least-squares technique using the SHELXL-2018/3[33] program. All non-hydrogen atoms were refined with anisotropic thermal parameters, while all hydrogen atoms were placed using AFIX instructions.

Compound **4a**(**a**): $C_{128}H_{96}N_2O_4$·2(toluene)·(hexane). Single crystals for X-ray diffraction were grown from toluene/hexane solution. The diffraction data are summarized in Table S1.

Compound **4a**(**b**): $C_{128}H_{96}N_2O_4$·$CHCl_3$·(solvents). Single crystals for X-ray diffraction were grown from $CHCl_3$/MTBE solution. Accessible voids were found in the unit cell. Attempts to model the solvent molecules ($CHCl_3$, MTBE, and/or H_2O) were not successful due to heavy disorder of the molecules. The diffuse electron density associated with the solvent molecules was removed by the PLATON/SQUEEZE[34] program. The diffraction data are summarized in Table S2.

■ ASSOCIATED CONTENT

Supporting Information

The Supporting Information is available free of charge at https://pubs.acs.org/doi/10.1021/acs.joc.2c00086.

VT-NMR studies, copies of ^{1}H and ^{13}C NMR spectra of new compounds, 2D NMR spectra, the diffraction data, HRMS data of [2]rotaxanes, and X-ray data for **4a**(**a**) and **4a**(**b**) (PDF)

Accession Codes

CCDC 2119495−2119496 contain the supplementary crystallographic data for this paper. These data can be obtained free of charge via www.ccdc.cam.ac.uk/data_request/cif, or by emailing data_request@ccdc.cam.ac.uk, or by contacting The Cambridge Crystallographic Data Centre, 12 Union Road, Cambridge CB2 1EZ, UK; fax: +44 1223 336033.

■ AUTHOR INFORMATION

Corresponding Author

Shinichi Saito − *Department of Chemistry, Faculty of Science, Tokyo University of Science, Tokyo 162-8601, Japan;* orcid.org/0000-0001-8520-1116; Email: ssaito@rs.tus.ac.jp

Authors

Yusuke Kawasaki − *Department of Chemistry, Faculty of Science, Tokyo University of Science, Tokyo 162-8601, Japan*

Showkat Rashid − *Department of Chemistry, Faculty of Science, Tokyo University of Science, Tokyo 162-8601, Japan*

Katsuhiko Ikeyatsu − *Department of Chemistry, Faculty of Science, Tokyo University of Science, Tokyo 162-8601, Japan*

Yuichiro Mutoh − *Department of Chemistry, Faculty of Science, Tokyo University of Science, Tokyo 162-8601, Japan;* Present Address: Center for Sustainable Resource Science, RIKEN, 2-1 Hirosawa, Wako, Saitama 351-0198, Japan; orcid.org/0000-0002-5254-9383

Yusuke Yoshigoe − *Department of Chemistry, Faculty of Science, Tokyo University of Science, Tokyo 162-8601, Japan*

Shoko Kikkawa − *Faculty of Pharmaceutical Sciences, Toho University, Funabashi, Chiba 274-8510, Japan;* orcid.org/0000-0002-9390-5671

Isao Azumaya − *Faculty of Pharmaceutical Sciences, Toho University, Funabashi, Chiba 274-8510, Japan;* orcid.org/0000-0002-6651-2768

Shoichi Hosoya − *Research Center for Medical and Dental Sciences, Tokyo Medical and Dental University, Tokyo 113-8510, Japan*

Complete contact information is available at: https://pubs.acs.org/10.1021/acs.joc.2c00086

Notes

The authors declare no competing financial interest.

https://doi.org/10.1021/acs.joc.2c00086
J. Org. Chem. 2022, 87, 5744−5759

■ ACKNOWLEDGMENTS

This work was supported by JSPS KAKENHI grant number JP19K05442 and the Science Research Promotion Fund. We thank Dr. Yoshitaka Tsuchido and Professor Hidetoshi Kawai (Tokyo University of Science) for the observation of the EXSY NMR spectra.

■ REFERENCES

(1) (a) Tian, H.; Wang, Q.-C. Recent progress on switchable rotaxanes. *Chem. Soc. Rev.* **2006**, *35*, 361−374. (b) Loeb, S. J. Rotaxanes as ligands: from molecules to materials. *Chem. Soc. Rev.* **2007**, *36*, 226−235. (c) Xue, M.; Yang, Y.; Chi, X.; Yan, X.; Huang, F. Development of Pseudorotaxanes and Rotaxanes: From Synthesis to Stimuli−Responsive Motions to Applications. *Chem. Rev.* **2015**, *115*, 7398−7501. (d) Bruns, C. J.; Stoddart, J. F. *The Nature of the Mechanical Bond: From Molecules to Machines*; Wiley: Hoboken, 2016. (e) Lewis, J. E. M.; Beer, P. D.; Loeb, S. J.; Goldup, S. M. Metal ions in the synthesis of interlocked molecules and materials. *Chem. Soc. Rev.* **2017**, *46*, 2577−2591. (f) Gao, W.-X.; Feng, H.-J.; Guo, B.-B.; Lu, Y.; Jin, G.-X. Coordination-Directed Construction of Molecular Links. *Chem. Rev.* **2020**, *120*, 6288−6325.

(2) Dietrich-Buchecker, C. O.; Sauvage, J. P.; Kern, J. M. Templated Synthesis of Interlocked Macrocyclic Ligands−the catenands. *J. Am. Chem. Soc.* **1984**, *106*, 3043−3045.

(3) Wu, C.; Lecavalier, P. R.; Shen, Y. X.; Gibson, H. W. Synthesis of a Rotaxane via the Template Method. *Chem. Mater.* **1991**, *3*, 569−572.

(4) (a) Fuller, A.-M. L.; Leigh, D. A.; Lusby, P. J.; Slawin, A. M. Z.; Walker, D. B. Selecting topology and connectivity through metal-directed macrocyclization reactions: A square planar palladium [2]catenate and two noninterlocked isomers. *J. Am. Chem. Soc.* **2005**, *127*, 12612−12619. (b) Leigh, D. A.; Lusby, P. J.; McBurney, R. T.; Morelli, A.; Slawin, A. M. Z.; Thomson, A. R.; Walker, D. B. Getting Harder: Cobalt(III)-Template Synthesis of Catenanes and Rotaxanes. *J. Am. Chem. Soc.* **2009**, *131*, 3762−3771. (c) Collin, J.-P.; Durola, F.; Frey, J.; Heitz, V.; Reviriego, F.; Sauvage, J.-P.; Trolez, Y.; Rissanen, K. Templated Synthesis of Cyclic [4]Rotaxanes Consisting of Two Stiff Rods Threaded through Two Bis-macrocycles with a Large and Rigid Central Plate as Spacer. *J. Am. Chem. Soc.* **2010**, *132*, 6840−6850. (d) Joosten, A.; Trolez, Y.; Collin, J.-P.; Heitz, V.; Sauvage, J.-P. Copper(I)-Assembled [3]Rotaxane Whose Two Rings Act as Flapping Wings. *J. Am. Chem. Soc.* **2012**, *134*, 1802−1809.

(5) Crowley, J. D.; Goldup, S. M.; Lee, A.-L.; Leigh, D. A.; McBurney, R. T. Active metal template synthesis of rotaxanes, catenanes and molecular shuttles. *Chem. Soc. Rev.* **2009**, *38*, 1530−1541.

(6) Aucagne, V.; Hänni, K. D.; Leigh, D. A.; Lusby, P. J.; Walker, D. B. Catalytic "click" rotaxanes: A substoichiometric metal-template pathway to mechanically interlocked architectures. *J. Am. Chem. Soc.* **2006**, *128*, 2186−2187.

(7) (a) Saito, S.; Takahashi, E.; Nakazono, K. Synthesis of [2]rotaxanes by the catalytic reactions of a macrocyclic copper complex. *Org. Lett.* **2006**, *8*, 5133−5136. (b) Yamashita, Y.; Mutoh, Y.; Yamasaki, R.; Kasama, T.; Saito, S. Synthesis of [3]Rotaxanes that Utilize the Catalytic Activity of a Macrocyclic Phenanthroline−Cu Complex: Remarkable Effect of the Length of the Axle Precursor. *Chem.—Eur. J.* **2015**, *21*, 2139−2145. (c) Saito, S.; Ohkubo, T.; Yamazaki, Y.; Yokoyama, T.; Mutoh, Y.; Yamasaki, R.; Kasama, T. A Macrocyclic Phenanthroline−Copper Complex with Less Steric Hindrance: Synthesis, Structure, and Application to the Synthesis of a [2]Rotaxane. *Bull. Chem. Soc. Jpn.* **2015**, *88*, 1323−1330. (d) Saito, S.; Hirano, Y.; Mutoh, Y.; Kasama, T. Synthesis of a Homochiral [2]Rotaxane from a BINOL-derived Macrocyclic Phenanthroline. *Chem. Lett.* **2015**, *44*, 1509−1511. (e) Hayashi, R.; Mutoh, Y.; Kasama, T.; Saito, S. Synthesis of [3]Rotaxanes by the Combination of Copper-Mediated Coupling Reaction and Metal-Template Approach. *J. Org. Chem.* **2015**, *80*, 7536−7546. (f) Mochizuki, Y.; Ikeyatsu, K.; Mutoh, Y.; Hosoya, S.; Saito, S. Synthesis of Mechanically Planar Chiral *rac*-[2]Rotaxanes by Partitioning of an Achiral [2]Rotaxane: Stereoinversion Induced by Shuttling. *Org. Lett.* **2017**, *19*, 4347−4350. (g) Yamazaki, Y.; Mutoh, Y.; Saito, S. Synthesis of Interlocked Compounds by Utilizing Bond-forming Reactions Mediated by Macrocyclic Phenanthroline-Cu Complexes. *Chem. Lett.* **2017**, *46*, 904−912. (h) Yamashita, Y.; Saito, Y.; Kikkawa, S.; Mutoh, Y.; Hosoya, S.; Azumaya, I.; Saito, S. Evaluation of the Steric Bulk of Substituents Utilizing the Shuttling Behavior of [2]Rotaxanes with *N*-Arylpyrrole Moieties. *Eur. J. Org. Chem.* **2019**, *2019*, 3412−3420.

(8) (a) Movsisyan, L. D.; Kondratuk, D. V.; Franz, M.; Thompson, A. L.; Tykwinski, R. R.; Anderson, H. L. Synthesis of Polyyne Rotaxanes. *Org. Lett.* **2012**, *14*, 3424−3426. (b) Sahnoune, H.; Baranová, Z.; Bhuvanesh, N.; Gladysz, J. A.; Halet, J.-F. A Metal-Capped Conjugated Polyyne Threaded through a Phenanthroline-Based Macrocycle. Probing beyond the Mechanical Bond to Interactions in Interlocked Molecular Architectures. *Organometallics* **2013**, *32*, 6360−6367. (c) Baranová, Z.; Amini, H.; Bhuvanesh, N.; Gladysz, J. A. Rotaxanes Derived from Dimetallic Polyynediyl Complexes: Extended Axles and Expanded Macrocycles. *Organometallics* **2014**, *33*, 6746−6749. (d) Movsisyan, L. D.; Peeks, M. D.; Greetham, G. M.; Towrie, M.; Thompson, A. L.; Parker, A. W.; Anderson, H. L. Photophysics of Threaded sp-Carbon Chains: The Polyyne is a Sink for Singlet and Triplet Excitation. *J. Am. Chem. Soc.* **2014**, *136*, 17996−18008. (e) Franz, M.; Januszewski, J. A.; Wendinger, D.; Neiss, C.; Movsisyan, L. D.; Hampel, F.; Anderson, H. L.; Görling, A.; Tykwinski, R. R. Cumulene Rotaxanes: Stabilization and Study of [9]Cumulenes. *Angew. Chem., Int. Ed.* **2015**, *54*, 6645−6649. (f) Movsisyan, L. D.; Franz, M.; Hampel, F.; Thompson, A. L.; Tykwinski, R. R.; Anderson, H. L. Polyyne Rotaxanes: Stabilization by Encapsulation. *J. Am. Chem. Soc.* **2016**, *138*, 1366−1376. (g) Kohn, D. R.; Movsisyan, L. D.; Thompson, A. L.; Anderson, H. L. Porphyrin−Polyyne [3]- and [5]Rotaxanes. *Org. Lett.* **2017**, *19*, 348−351. (h) Franz, M.; Januszewski, J. A.; Hampel, F.; Tykwinski, R. R. [3]Rotaxanes with Mixed Axles: Polyynes and Cumulenes. *Eur. J. Org. Chem.* **2019**, *2019*, 3503−3512. (i) Woltering, S. L.; Gawel, P.; Christensen, K. E.; Thompson, A. L.; Anderson, H. L. Photochemical Unmasking of Polyyne Rotaxanes. *J. Am. Chem. Soc.* **2020**, *142*, 13523−13532.

(9) Lahlali, H.; Jobe, K.; Watkinson, M.; Goldup, S. M. Macrocycle Size Matters: "Small" Functionalized Rotaxanes in Excellent Yield Using the CuAAC Active Template Approach. *Angew. Chem., Int. Ed.* **2011**, *50*, 4151−4155.

(10) Bonardi, F.; Halza, E.; Walko, M.; Du Plessis, F.; Nouwen, N.; Feringa, B. L.; Driessen, A. J. M. Probing the SecYEG translocation pore size with preproteins conjugated with sizable rigid spherical molecules. *Proc. Natl. Acad. Sci. U.S.A.* **2011**, *108*, 7775−7780.

(11) Leas, D. A.; Dong, Y.; Vennerstrom, J. L.; Stack, D. E. One-Pot, Metal-Free Conversion of Anilines to Aryl Bromides and Iodides. *Org. Lett.* **2017**, *19*, 2518−2521.

(12) Rodríguez, J. G.; Tejedor, J. L.; La Parra, T.; Díaz, C. Synthesis of conjugated 2,7-bis(trimethylsilylethynyl)-(phenylethynyl)$_n$fluoren-9-one and 9-(*p*-methoxyphenyl)-9-methyl derivatives: optical properties. *Tetrahedron* **2006**, *62*, 3355−3361.

(13) Bandgar, B. P.; Bettigeri, S. V.; Phopase, J. Palladium catalyzed ligand-free Suzuki cross-coupling reactions of benzylic halides with aryl boronic acids under mild conditions. *Tetrahedron Lett.* **2004**, *45*, 6959−6962.

(14) Lembo, A.; Tagliatesta, P.; Guldi, D. M.; Wielopolski, M.; Nuccetelli, M. Porphyrin−β-Oligo-Ethynylenephenylene−[60]-Fullerene Triads: Synthesis and Electrochemical and Photophysical Characterization of the New Porphyrin−Oligo-PPE−[60]Fullerene Systems. *J. Phys. Chem. A* **2009**, *113*, 1779−1793.

(15) Moss, K. C.; Bourdakos, K. N.; Bhalla, V.; Kamtekar, K. T.; Bryce, M. R.; Fox, M. A.; Vaughan, H. L.; Dias, F. B.; Monkman, A. P. Tuning the Intramolecular Charge Transfer Emission from Deep Blue to Green in Ambipolar Systems Based On Dibenzothiophene *S,S*-Dioxide by Manipulation of Conjugation and Strength of the Electron Donor Units. *J. Org. Chem.* **2010**, *75*, 6771−6781.

https://doi.org/10.1021/acs.joc.2c00086
J. Org. Chem. 2022, 87, 5744−5759

(16) Suzuki, T.; Ota, Y.; Ri, M.; Bando, M.; Gotoh, A.; Itoh, Y.; Tsumoto, H.; Tatum, P. R.; Mizukami, T.; Nakagawa, H.; Iida, S.; Ueda, R.; Shirahige, K.; Miyata, N. Rapid Discovery of Highly Potent and Selective Inhibitors of Histone Deacetylase 8 Using Click Chemistry to Generate Candidate Libraries. *J. Med. Chem.* **2012**, *55*, 9562−9575.
(17) Ton, Q. C.; Bolte, M. A co-crystal of 1,10-phenanthroline and chloroform. *Acta Crystallogr., Sect. E: Struct. Rep. Online* **2005**, *E61*, O1406−O1407.
(18) If the ring component is located in a specific position, the signals of a limited number of protons bound to the axle component would be shifted significantly upon the formation of the rotaxane. This was not observed in our study.
(19) A reviewer pointed out the possible interaction between the phenanthroline moiety and the stoppers (triarylmethyl group). The interaction, if any, would not be strong. If this type of interaction is strong, the triarymethyl group would be magnetically non-equivalent. The observed spectra at rt shows that the triarylmethyl groups are magnetically equivalent. The observed equivalent signals of the triarylmethyl groups of **4c** at low temperature (see Figure S1) supports the idea that the interaction between the phenanthroline moiety and the stoppers is not strong.
(20) Most of the signals were readily assigned by the chemical shifts, integral values, and the coupling patterns. Some ambiguous signals were assigned by analyzing ^{1}H−^{1}H COSY NMR spectra of the compounds. See Supporting Information for details.
(21) Here, the term "distance" is used to describe the average of the distance between the phenanthroline moiety and the axle moiety in all conformers of the [2]rotaxane.
(22) (a) Winn, J.; Pinczewska, A.; Goldup, S. M. Synthesis of a Rotaxane Cu^{I} Triazolide under Aqueous Conditions. *J. Am. Chem. Soc.* **2013**, *135*, 13318−13321. (b) Bordoli, R. J.; Goldup, S. M. An Efficient Approach to Mechanically Planar Chiral Rotaxanes. *J. Am. Chem. Soc.* **2014**, *136*, 4817−4820. (c) de Juan, A.; Lozano, D.; Heard, A. W.; Jinks, M. A.; Suarez, J. M.; Tizzard, G. J.; Goldup, S. M. A chiral interlocking auxiliary strategy for the synthesis of mechanically planar chiral rotaxanes. *Nat. Chem.* **2022**, *14*, 179−187.
(23) Though the observed difference of the chemical shifts was large in the triazole rotaxane **4i** and the components, this does not necessarily imply that hydrogen bond in **4i** is stronger than those in other rotaxanes. The magnitude of the difference of the chemical shifts could also be affected by the structure incorporated in the axle moiety.
(24) The comparison of ^{1}H NMR spectra in other polar solvents turned out to be problematic. Ring component **1** was insoluble in CD_3OD and almost insoluble in CD_3CN. Rotaxane **4f** was insoluble in CD_3CN. In acetone-d_6, compound **1** and the axle component **17f** were soluble but the rotaxane **4f** was not soluble. The result may imply that **1** and **17f** formed hydrogen bond with acetone but the rotaxane **4f** could not interact with acetone via hydrogen bond. We thank the reviewer for suggesting this experiment.
(25) Attempted NOESY analysis of **4f** was not successful: no cross peak between the axle and ring components was detected (see Supporting Information).
(26) For examples, see, (a) Garaudée, S.; Silvi, S.; Venturi, M.; Credi, A.; Flood, A. H.; Stoddart, J. F. Shuttling Dynamics in an Acid−Base-Switchable [2]Rotaxane. *ChemPhysChem* **2005**, *6*, 2145−2152. (b) Hmadeh, M.; Fahrenbach, A. C.; Basu, S.; Trabolsi, A.; Benítez, D.; Li, H.; Albrecht-Gary, A. M.; Elhabiri, M.; Stoddart, J. F. Electrostatic Barriers in Rotaxanes and Pseudorotaxanes. *Chem.—Eur. J.* **2011**, *17*, 6076−6087. (c) Young, P. G.; Hirose, K.; Tobe, Y. Axle Length Does Not Affect Switching Dynamics in Degenerate Molecular Shuttles with Rigid Spacers. *J. Am. Chem. Soc.* **2014**, *136*, 7899−7906. (d) Matsuoka, Y.; Mutoh, Y.; Azumaya, I.; Kikkawa, S.; Kasama, T.; Saito, S. Synthesis and Shuttling Behavior of [2]-Rotaxanes with a Pyrrole Moiety. *J. Org. Chem.* **2016**, *81*, 3479−3487.
(27) This assumption is based on the analysis of the temperature-chemical shift profile of **4h**. The attempted detection of the other signal by EXSY NMR analysis of **4h** at 180 K was unsuccessful (see Supporting Information).
(28) See Supporting Information for details.
(29) Detailed quantitative analysis was not possible because of the overlap of the N−H signals with other signals.
(30) Attempted EXSY NMR analysis of **4f** at 193 K was unsuccessful. No cross peak which would correspond to the chemical exchange of the NH protons was observed (see Supporting Information).
(31) Kabuto, C.; Akine, S.; Nemoto, T.; Kwon, E. Release of Software (Yadokari-XG 2009) for Crystal Structure Analyses. *J. Crystallogr. Soc. Jpn.* **2009**, *51*, 218−224 (in Japanese).
(32) Sheldrick, G. M. SHELXT − Integrated Space-Group and Crystal-Structure Determination. *Acta Crystallogr., Sect. A: Found. Adv.* **2015**, *71*, 3−8.
(33) (a) Sheldrick, G. M. Crystal Structure Refinement with SHELXL. *Acta Crystallogr., Sect. C: Struct. Chem.* **2015**, *71*, 3−8.
(34) Spek, A. L. PLATON SQUEEZE: A Tool for the Calculation of the Disordered Solvent Contribution to the Calculated Structure Factors. *Acta Crystallogr., Sect. C: Struct. Chem.* **2015**, *71*, 9−18.

https://doi.org/10.1021/acs.joc.2c00086
J. Org. Chem. 2022, 87, 5744−5759